

Geochemistry, Geophysics, Geosystems®







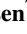






RESEARCH ARTICLE

10.1029/2024GC011837

The Enigmatic Pockmarks of the Sandy Southeastern North Sea

Key Points:

- Pockmarks in the German Bight form in sandy environments and are likely not related to fluid venting
- Pockmarks in sandy sediments are shallow in depth, large in area and short-lived structures compared to muddy host sediments
- Despite the widespread occurrence of pockmarks in the southeastern North Sea, the processes leading to their formation remain unclear

Christoph Böttner^{1,2} , Jasper J. L. Hoffmann^{3,4} , Daniel Unverricht^{1,5} , Mark Schmidt⁶ , Timo Spiegel⁶ , Jacob Geersen⁷ , Thomas Harald Müller⁶ , Jens Karstens⁶ , Katrine Juul Andresen² , Lasse Sander³ , Jens Schneider von Deimling¹ , and Christopher Schmidt⁶ 

¹Institute of Geosciences, Kiel University, Kiel, Germany, ²Department of Geoscience, Aarhus University, Aarhus, Denmark, ³Coastal Ecology, Alfred-Wegener-Institute, Helmholtz Centre for Polar and Marine Research, List, Germany, ⁴Department of Geosciences, Marine Geology and Seafloor Surveying Group, University of Malta, Msida, Malta, ⁵Landesamt für Umwelt des Landes Schleswig-Holstein, Flintbek, Germany, ⁶GEOMAR Helmholtz Centre for Ocean Research, Kiel, Germany, ⁷Leibniz Institute for Baltic Sea Research Warnemuende, Rostock, Germany

Correspondence to:

C. Böttner,
Christoph.Boettner@geo.au.dk

Citation:

Böttner, C., Hoffmann, J. J. L., Unverricht, D., Schmidt, M., Spiegel, T., Geersen, J., et al. (2024). The enigmatic pockmarks of the sandy southeastern North Sea. *Geochemistry, Geophysics, Geosystems*, 25, e2024GC011837. <https://doi.org/10.1029/2024GC011837>

Received 27 AUG 2024

Accepted 29 OCT 2024

Author Contributions:

Conceptualization: Christoph Böttner, Jasper J. L. Hoffmann, Mark Schmidt, Christopher Schmidt

Data curation: Christoph Böttner, Jasper J. L. Hoffmann, Daniel Unverricht, Mark Schmidt, Jens Karstens, Christopher Schmidt

Formal analysis: Christoph Böttner, Jasper J. L. Hoffmann, Daniel Unverricht, Mark Schmidt, Timo Spiegel, Jacob Geersen, Thomas Harald Müller, Jens Karstens, Katrine Juul Andresen

Funding acquisition: Christoph Böttner, Christopher Schmidt

Investigation: Christoph Böttner, Jasper J. L. Hoffmann, Daniel Unverricht, Mark Schmidt, Timo Spiegel, Jacob Geersen, Thomas Harald Müller, Jens Karstens, Katrine Juul Andresen,

Abstract Natural seafloor depressions, known as pockmarks, are common subaqueous geomorphological features found from the deep ocean trenches to shallow lakes. Pockmarks can form rapidly or over millions of years and have a large variety of shapes created and maintained by a large variety of mechanisms. In the sandy sediments of the southeastern North Sea, abundant shallow pockmarks are ubiquitous and occur at shallow water depths (<50 m). Their formation has previously been linked to methane seepage from the seafloor. Here, we characterize over 50,000 pockmarks based on their morphology, geochemical signature, and the subsurface pre-conditions using a new integrated geoscientific data set, combining geophysical and sedimentological data with geochemical porewater and oceanographic analysis. We test whether the methane seepage is indeed responsible for pockmark formation. However, our data suggest that neither the seepage of light hydrocarbons nor groundwater is driving pockmark formation. Because of this lack of evidence for fluid seepage, we favor the previously suggested biotic formation but also discuss positive feedback mechanisms in ocean bottom currents as a formation process. Based on a comparison of pockmarks to the central and southeastern North Sea, we find that local lithology significantly affects pockmark morphology. Muddy lithologies favor the formation of larger, long-lived structures, while sandy lithologies lead to short-lived, small-scale structures that are large in area but with shallow incision depth. We conclude that pockmarks in sandy environments might have been overlooked globally due to their shallow incision depth and recommend reevaluating the role of hydrocarbon ebullition in pockmark formation.

Plain Language Summary Pockmarks are natural depressions on the seafloor, found everywhere from deep oceans to shallow lakes. These underwater features can form quickly or over millions of years, sometimes reaching impressive sizes—tens of meters deep and kilometers wide. Pockmarks are created by different processes depending on where they are found, but they are often linked to the release of gases such as methane from the seafloor. In the southeastern North Sea, thousands of shallow pockmarks have been discovered in sandy areas less than 50 m deep. Initially thought to be caused by methane gas leaks, our research shows this is unlikely. We studied over 50,000 pockmarks using geological, chemical, and oceanographic data and found little evidence that methane or groundwater seepage is responsible. Instead, these pockmarks are more likely created by either marine animals such as harbor porpoises or turbulent ocean currents. We also found that the grainsize of the sediment greatly affects pockmark morphology and lifespan. In muddy areas, pockmarks are larger and longer-lasting, whereas in sandy areas, they are shallower and shorter-lived. Our findings suggest that many pockmarks in sandy environments may have been overlooked due to their shallow depth. We recommend reconsidering the role of methane in pockmark formation.

© 2024 The Author(s). Geochemistry, Geophysics, Geosystems published by Wiley Periodicals LLC on behalf of American Geophysical Union.

This is an open access article under the terms of the [Creative Commons Attribution License](https://creativecommons.org/licenses/by/4.0/), which permits use, distribution and reproduction in any medium, provided the original work is properly cited.

1. Introduction

Pockmarks are common geologic features that form on the seafloor. In marine geology, the term “pockmark” was introduced by King and MacLean (1970) based on findings from the Nova Scotian shelf describing (semi-) circular depressions on the seafloor. Since then, pockmarks have been found in almost all subaqueous geologic settings spanning from deep ocean trenches to shallow lakes (Bussmann et al., 2013; Dimitrov &

Lasse Sander, Jens Schneider von Deimling, Christopher Schmidt
Methodology: Mark Schmidt, Thomas Harald Müller

Project administration:

Christoph Böttner, Jasper J. L. Hoffmann, Daniel Unverricht, Christopher Schmidt

Resources: Jasper J. L. Hoffmann, Mark Schmidt, Jens Karstens, Katrine Juul Andresen, Lasse Sander, Jens Schneider von Deimling, Christopher Schmidt

Software: Jens Schneider von Deimling

Supervision: Christoph Böttner

Validation: Jasper J. L. Hoffmann, Daniel Unverricht, Mark Schmidt, Timo Spiegel, Jacob Geersen, Thomas Harald Müller

Visualization: Christoph Böttner, Jasper J. L. Hoffmann, Daniel Unverricht, Mark Schmidt

Writing – original draft:

Christoph Böttner, Jasper J. L. Hoffmann, Daniel Unverricht, Mark Schmidt, Christopher Schmidt

Writing – review & editing:

Christoph Böttner, Jasper J. L. Hoffmann, Daniel Unverricht, Mark Schmidt, Timo Spiegel, Jacob Geersen, Thomas Harald Müller, Jens Karstens, Katrine Juul Andresen, Lasse Sander, Jens Schneider von Deimling, Christopher Schmidt

Woodside, 2003; Hillman et al., 2023; Judd & Hovland, 2009; Kelley et al., 1994; Reusch et al., 2015; Watson et al., 2020; Webb et al., 2009). According to Judd and Hovland (2009) “the key factors that distinguish pockmarks from other morphologically similar features are that they are erosive, and that the eroding agent comes from beneath the seabed.” As many studies worldwide refer to seafloor depressions as pockmarks although their origin remains unknown (Hillman et al., 2023; Hoffman et al., 2019; Paull et al., 2002), and to be consistent with previous terminology used in the North Sea, we will use the term pockmark here to describe seafloor depressions of unknown origin (Krämer et al., 2017). Pockmarks can be meters to hundreds of meters in diameter and meters to tens of meters in depth (Davy et al., 2010; Micalef et al., 2022). They may form over geologic time scales (thousand to millions of years) or short time periods such as hours, days, or weeks (Andresen et al., 2021; Böttner et al., 2019; Dumke et al., 2014; Hovland et al., 2002; Paull et al., 2002). Pockmarks may be active and release fluids continuously or intermittently (Böttner et al., 2019; Karstens et al., 2022) but can also be completely inactive (Lundsten et al., 2024; Paull et al., 2002). Because of this diverse occurrence, morphological dynamics, size, and character, pockmarks are likely formed and maintained by a large variety of mechanisms.

The primary model for pockmark formation is the venting of hydrocarbons, that is, oil and gas (Judd & Hovland, 2009). The study of pockmarks has largely been driven by the oil and gas industry to generate new knowledge on the potential deep hydrocarbon sources that might have fueled pockmark formation (Judd & Hovland, 2009). Pockmarks are often distinct morphological features that can be used to detect and characterize subsurface fluid flow systems and/or hydrocarbon plays (Böttner et al., 2020; Feldens et al., 2016; Judd & Hovland, 2009). However, the dominance of this model may spuriously lead to the interpretation that all pockmarks are associated with hydrocarbon venting (Paull et al., 2002). Pockmarks may also form and/or be maintained by other mechanisms such as groundwater discharge or pore-water expulsion (Andresen et al., 2008, 2021; Chenrai & Huuse, 2017; Hoffmann et al., 2020, 2023; Whiticar & Werner, 1981). Another valid explanation for the formation of depressions on the seafloor arises from agents coming from above, such as marine vertebrates or other benthic fauna known to excavate seafloor depressions (up to meters deep), which could be termed pockmarks as well (Baird, 1988; Hein & Syvitski, 1989; Johnson & Nelson, 1984; Mueller, 2015; Purser et al., 2022; Schneider von Deimling et al., 2023; Wall et al., 2011; Wright & Jones, 2006). Regardless of their formation, pockmarks have a strong impact on the local environments, morpho-dynamics, biogeochemistry, and ecology (Judd & Hovland, 2009).

In this study, we investigate the origins and morphological characteristics of suddenly appearing and disappearing pockmarks in the southeastern North Sea (Figure 1). These pockmarks can be found over a wide area (>1,000 km²) and occur at great density (>1,200 per square kilometer), which results in an exceptional number of pockmarks (>300,000) (Krämer et al., 2017). The pockmarks occur in water depths ranging from 25 to 40 m and are typically only 0.2 m deep but 10–20 m wide (Krämer et al., 2017). In this area, the seafloor sediments consist of fine to medium sands with a low mud content (<5%) (Coughlan et al., 2018). Strong tidal currents within this part of the North Sea make it a morphodynamically active environment. The approximately 45–50 m deep channel of the (Paleo-) Elbe estuary bounds the survey area in the southwest (Özmaral et al., 2022; Papenmeier & Hass, 2020).

So far, there are limited explanations on the formation of these pockmarks. Krämer et al. (2017) proposed a model for massive methane release (5,000 t/a) during storm events. They further proposed a model where tidal currents excavate the depressions started by the methane release. Thus, pockmarks are formed by hydrocarbon release and supported by tidal currents. This hypothesis was further investigated using advanced numerical models (Gupta et al., 2022) that showed that pockmark formation was indeed feasible during large storm events, but only if there were sufficient dissolved pore water gases of about 50% saturation available. However, so far, only limited proof of shallow gas accumulations is available from the southeastern North Sea. In contrast to these fluid venting hypotheses, Schneider von Deimling et al. (2023) proposed that marine vertebrates could initiate pits at the seafloor during their hunt for prey, which are subsequently widened by tidal currents. In order to test the different formation mechanisms, we present a new integrated geoscientific data set from the German Bight, southeastern North Sea. Geophysical, geological, sedimentological, and geochemical methods are combined to investigate the enigmatic case of the pockmarks formed in fine sands. In total, we characterize over 50,000 pockmarks found in this study based on their morphological expression on the seafloor, geochemical signature, and the subsurface pre-conditions. Additionally, we use time-lapse bathymetric surveys where we resurveyed a pockmark area four times over the course of 1 year to determine the environmental factors leading to the periodic vanishing and reappearance. Subsequently, we discuss the potential formation mechanisms of pockmarks in the southeastern

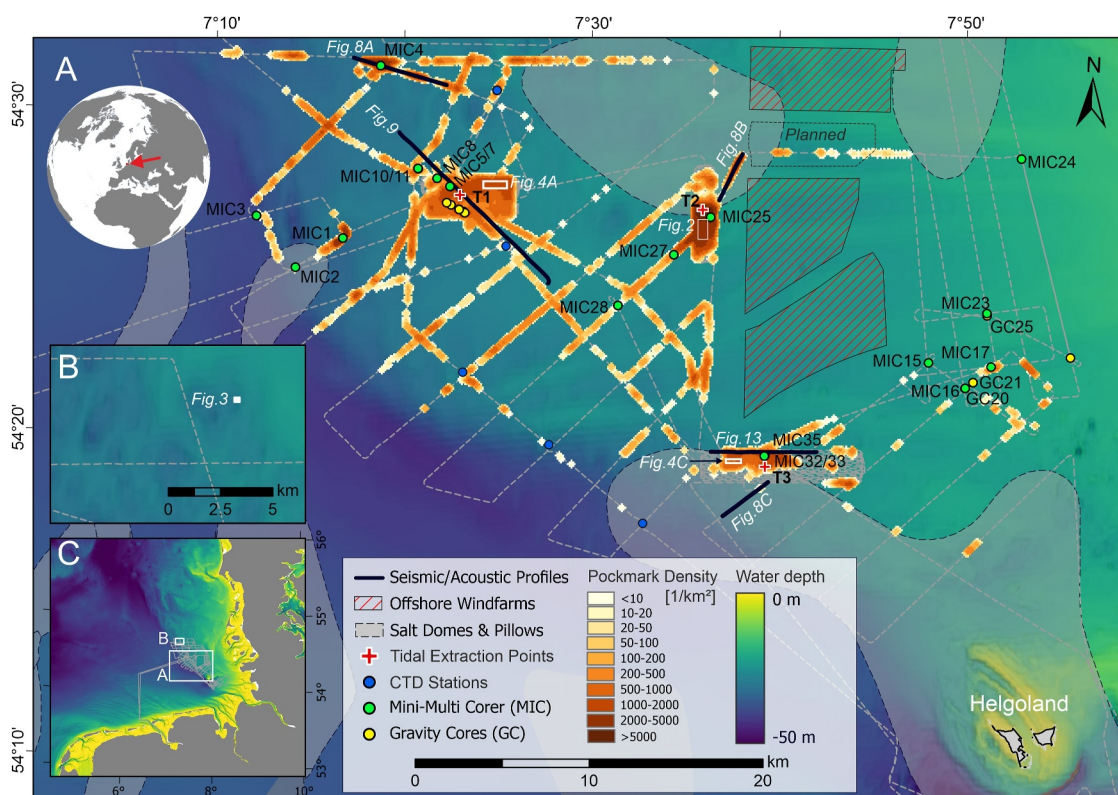


Figure 1. Bathymetric map of the southeastern North Sea. (a) Overview map showing the focus area of the MSM99/2 static data set with pockmark density as overlay. Seismic and subbottom echosounder profile locations are indicated with black lines. Red crosses are marking tidal and ocean current extraction points (red), while dots indicate the locations of mini-multi corer (green), CTD stations (blue), and gravity cores (yellow). Samples used for geochemical analyses are labeled. Salt domes and pillows are shown in transparent gray areas with dashed lines. (b) The time-lapse survey area (white box) is shown in Figure 3. (c) Overview Map of the German Bight of the southeastern North Sea with locations of (a) and (b) shown as white boxes.

North Sea and determine what differentiates the sandy pockmarks of the southeastern North Sea from those in the mud-rich sediment settings of the Central North Sea. This includes constraining the spatiotemporal genesis and evolution of these pockmarks and a morphological characterization of pockmarks formed in sandy substrates.

2. Methods

2.1. Hydroacoustic Data

Bathymetric data were acquired during R/V Heinke and R/V Maria S. Merian cruises HE576, HE588, HE592, HE602 and MSM99/2 using a hull mounted Kongsberg EM712 system (Table 1). The surveys were designed to provide high-resolution bathymetry with 0.5×0.5 m resolution. We processed the data using QPS Qimera and included elevation corrections (squat effect, tidal) and statistical evaluation of soundings (average over 0.5 m bin size) that increased the signal-to-noise ratio. The sound velocity profiles (CTD casts MSM99/2: 11; <https://doi.org/10.1029/2024GC011837>).

Table 1
List of Cruises Where Data Were Acquired

Cruise ID	Date	Reference
MSM99/2	2021-03-23–2021-04-04	https://doi.pangaea.de/10.1594/PANGAEA.933768
HE576	2021-05-06–2021-05-24	https://doi.pangaea.de/10.1594/PANGAEA.933817
HE588	2021-10-24–2021-11-04	https://doi.pangaea.de/10.1594/PANGAEA.940575
HE592	2022-02-23–2022-03-02	https://doi.pangaea.de/10.1594/PANGAEA.943948
HE602	2022-06-23–2022-07-06	https://doi.pangaea.de/10.1594/PANGAEA.947899

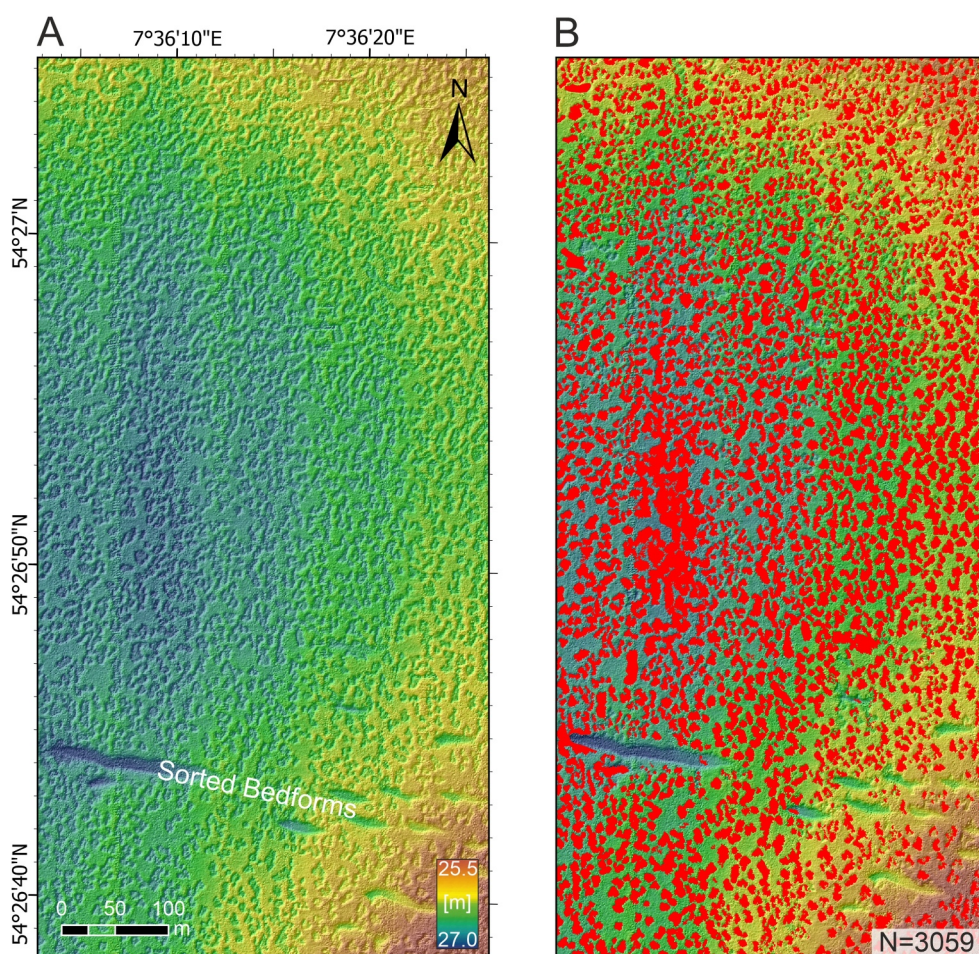


Figure 2. Bathymetric data set showing the pockmarks. (a) Uninterpreted bathymetric data set showing sorted bedforms and abundant pockmarks. (b) Semi-automated picking outlines the shapes of the pockmarks automatically and allows geomorphological analyses.

[org/10.1594/PANGAEA.967160](https://doi.org/10.1594/PANGAEA.967160)) for multibeam processing were measured daily to cover all parts of the survey area and the whole tidal cycle. In addition to the bathymetric data, we collected backscattering amplitudes of both the seafloor (snippets) and the water column (WCI).

For tidal corrections and ocean currents (speed and direction), we employed the numerical ocean forecasting system for the North Sea developed at the Federal Maritime and Hydrographic Agency (BSH). The circulation model “*BSH-HBMnoku*” accounts not only for tidal currents but also includes meteorological forcing (e.g., storm surges). It provides information on surface elevation, ocean currents, temperature, salinity, and ice conditions. The data can be obtained from the BSH via opmod@bsh.de.

We employed semi-automated picking of the pockmark shapes (methods see Böttner et al., 2019). The pockmark shapes are subsequently used to derive a wide range of geomorphological parameters. Picking works automatically but requires manual cleaning after picking to eliminate shapes that outline sorted bedforms and other unwanted features (Figure 2).

The shallow seismic stratigraphy was imaged by sub-bottom profiler data acquired during cruise MSM99/2 (2021/03/26–2021/04/05) using Parasound P70 with 4 kHz as the secondary low frequency to obtain seismic images of the upper sedimentary succession with remarkably high vertical resolution (<15 cm). We applied a frequency filter (2–6 kHz bandpass) and calculated the envelope within the seismic interpretation software IHS Kingdom. The penetration was particularly good and, in many parts, up to 20 m into the subsurface. We used the very high-resolution sub-bottom profiler data in addition to existing legacy data (2D seismic reflection, discussed

below) to characterize the subsurface and determine possible governing structures of the local geology that may explain the spatial distribution of pockmarks. Furthermore, we used the data to identify any fluids or fluid flow in the subsurface as the high-frequency system is highly sensitive to fluids or gases in the water column or within the pore space.

2.2. Seismic Data

Seismic acquisition was conducted during R/V Alkor cruise AL512 (2018/07/15–2018/07/26) and consisted of a 2D multi-channel reflection seismic system with a GI-airgun (15 in³ generator and 15 in³ injector) as source and a 212.5 m-long streamer with 136 hydrophone groups with a group spacing of 1.56 m for recording (Karstens et al., 2018). Seismic data processing included normal-moveout-correction, trace interpolation, bandpass filtering (corner frequencies: 50, 92, 680, and 800 Hz), multiple attenuation, and Stolt migration with a constant velocity of 1,500 m/s (Karstens et al., 2022). The resulting seismic data have a horizontal resolution of about 1.56 m (common midpoint spacing) and a vertical resolution of ~6 m at the seafloor ($\lambda/2$ criterion with dominant frequency of 125 Hz), decreasing downwards.

2.3. Sediment and Geochemical Sampling

Sediment samples were retrieved during Cruise MSM99/2 with a Mini-Multi Corer (MIC) equipped with 4 Perspex liners (10 × 60 cm). This sampling device is comparable to a multicorer, as undisturbed surface sediments and the overlying bottom waters are retrieved, but the MIC consists of fewer liners and has a smaller head weight. Between 10 and 24 cm of surface sediments were recovered during each deployment (see Figure 1). At selected locations, we also deployed a gravity corer for sediment sampling with a stainless steel tube, inner plastic liner, and 1.25 tons head-weight. Between 45 and 420 cm of sediment was recovered during deployments. Additionally, we used the Van-Veen grab sampler to collect undisturbed surface sediments (Schmidt et al., 2021).

Sediment coring stations of the survey area offshore Helgoland range from 20 to 50-m water depth (Figure 1). Only 7 out of 28 attempts of gravity coring were successful in terms of sediment recovery, reflecting the difficulty of sampling in a sandy environment without vibro-coring. In the case of the Mini-MIC, 26 out of 35 attempts successfully contained sediments. The grab sampler was used 10 times, containing sediment samples each time.

Sampling for grain size analyses was performed following the sediment description and first facies analysis. Each seismic facies was sampled at least once. For high resolution particle size measurements, we took 49 surface samples (1–2 g), which were measured using laser diffraction granulometry. First, sediment samples were treated with 10 ml of 30% hydrochloric acid and 10 ml 35% hydrogen peroxide to remove carbonate and organic content and then, samples were analyzed using a Malvern Mastersizer 2000.

Geochemical sediment sampling was performed in approximately 2-cm intervals for MIC sampling and 10 cm intervals for gravity core sampling. Surface sediment samples from the grab sampler were taken at approximately 1 and 5 cm depth. A defined volume of wet sediment was sampled into pre-weighed plastic cups for the determination of water content, porosity, and particulate organic matter content at GEOMAR (<https://www.geomar.de/en/mg-analytik>). Three milliliters of sediment were added to 20 ml headspace vials filled with 1.5 g NaCl and 9 ml of saturated NaCl solution, then crimped with silicone rubber stoppers and aluminum caps and stored after mixing for dissolved methane determination by using gas chromatography at GEOMAR (Sommer et al., 2009).

Pore-water samples from the cores were taken by Rhizon-extraction according to the method of Seeberg-Elverfeldt et al. (2005) at the same depth intervals as sediment samples. Samples for total alkalinity were analyzed onboard by titration of 1 ml pore water according to Grasshoff et al. (2009). Subsamples of pore water were stored at 4°C in plastic vials for subsequent analyses of chloride and sulfate by using ion chromatography at GEOMAR (<https://www.geomar.de/en/mg-analytik>).

3. Results

3.1. Multibeam Data

We use a time-lapse approach for a small area (300 × 300 m; Figure 3, see location Figure 1), as well as a static characterization of pockmarks over a larger area (Figure 4). In time-lapse surveys, we find pockmarks on the

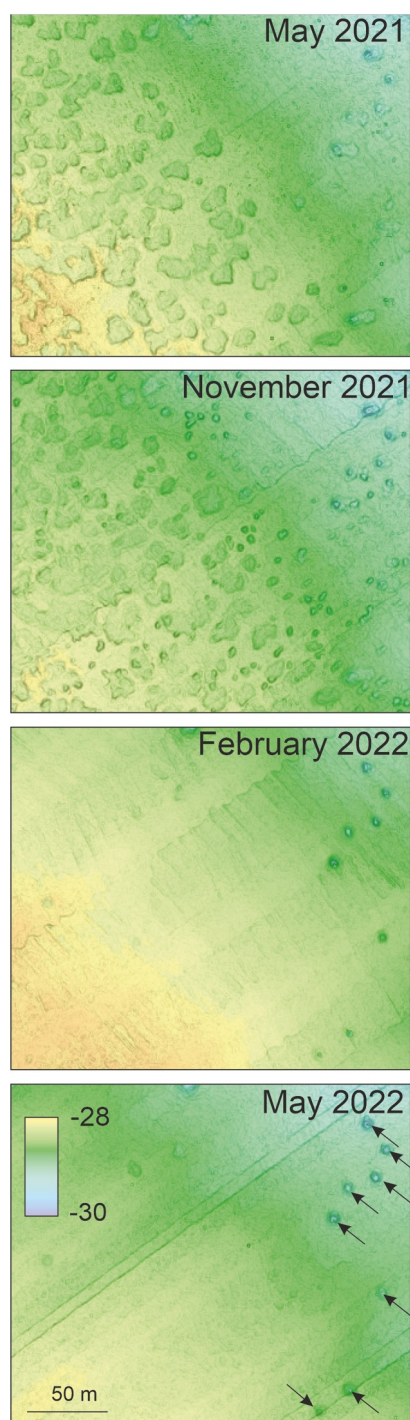


Figure 3. Time-lapse survey over the course of 1 year above a pockmark site. Pockmarks are visible during May 2021. In November 2021, new pockmarks emerge within the previous pockmark field but also in areas with a previous flat seafloor. In February and May 2022, no pockmarks were observed. Current scouring around the stones leads to persistent depressions indicated by arrows.

seafloor during surveys in May and November 2021, while the same region shows a flat featureless seafloor in February and May 2022 (Figure 3).

Our data show that pockmarks initiate as small circular “unit pockmarks” (Class 1, cf. Figure 4) that form within, but also in proximity to, previously existing complex pockmarks (Class 2, cf. Figure 4). The complex pockmarks resemble cauliflower if seen from above, which is why we term them “cauliflower pockmarks.” Both classes form and vanish over weeks to months. We find cauliflower-like pockmarks in our May 2021 data set, which are partly intermingled. In November 2021, the coalescence of the previously identified cauliflower pockmarks advanced and new, much smaller, unit pockmarks formed within and adjacent to the May 2021 pockmarks. While the cauliflower pockmarks grow in their spatial extent, their depth remains the same. During this fraying process, adjacent pockmarks may coalesce and form super-structures that can cover large areas ($\sim 9,400 \text{ m}^2$ compared to average area of 39.3 m^2) by connecting hundreds of cauliflower pockmarks. The time-lapse surveys additionally reveal that pockmark occurrence does not follow a periodical or seasonal cycle. Our data show that eight pockmarks remain stable and intact over the year (indicated by black arrows in Figure 3). These depressions, however, form because of scouring around individual boulders and are not considered as pockmarks here.

We use the large static data set (with $0.5 \times 0.5 \text{ m}$ of horizontal and $<15 \text{ cm}$ vertical resolution) for deriving geomorphological parameters of the pockmarks to find characteristics that allow a robust separation of the two classes (Figure 4). The qualitative assessment of pockmarks in our multibeam bathymetric data confirms the two classes of pockmarks (small unit pockmarks vs. wide complex cauliflower pockmarks). However, our data also show that a wide range of shapes exist in between the two classes.

Our semi-automated picking of the pockmarks and their shapes revealed a total of 51,827 individual pockmarks (Figure 5). The quantitative analyses of all identified pockmarks show an exceptionally low incision depth in comparison to their surrounding bathymetry ($27 \text{ cm} \pm 21 \text{ cm}$) with a close spacing of $13.1 \text{ m} \pm 8.7 \text{ m}$ in between (nearest neighboring pockmark distance). The median pockmark perimeter is about 26 m, and the median volume is $\sim 3 \text{ m}^3$ (see Figure 5). Because of the wide distribution over a broad range of values, the median values give a better description of most pockmarks in our data set (Figure 5).

From the qualitative assessment of pockmarks in our multibeam bathymetric data (Figures 3 and 4), we can distinguish two classes of pockmarks (small unit pockmarks vs. wide complex cauliflower pockmarks). These two classes are also supported by quantitative analyses of the pockmark shapes as well. For instance, circularity is a parameter that describes how close a shape is to a circle (Equation 1):

$$\text{Circularity} = 4\pi \cdot \frac{\text{Area}}{\text{Perimeter}^2} \quad (1)$$

The two classes can be easily distinguished by the circularity parameter. A Bayesian-Gaussian-Mixture-Model shows two distinct clusters that are separated at a circularity value of about 0.5. About 29% of the pockmarks (Class 1, $N = 14,914$; Figure 5f) show the typical characteristics of (semi-)circular depressions (“unit pockmarks”) with circularity values above 0.5 (1 equals perfect circular shape). About 71% of the pockmarks show a complex morphology (“cauliflower pockmarks”) with circularity values below 0.5

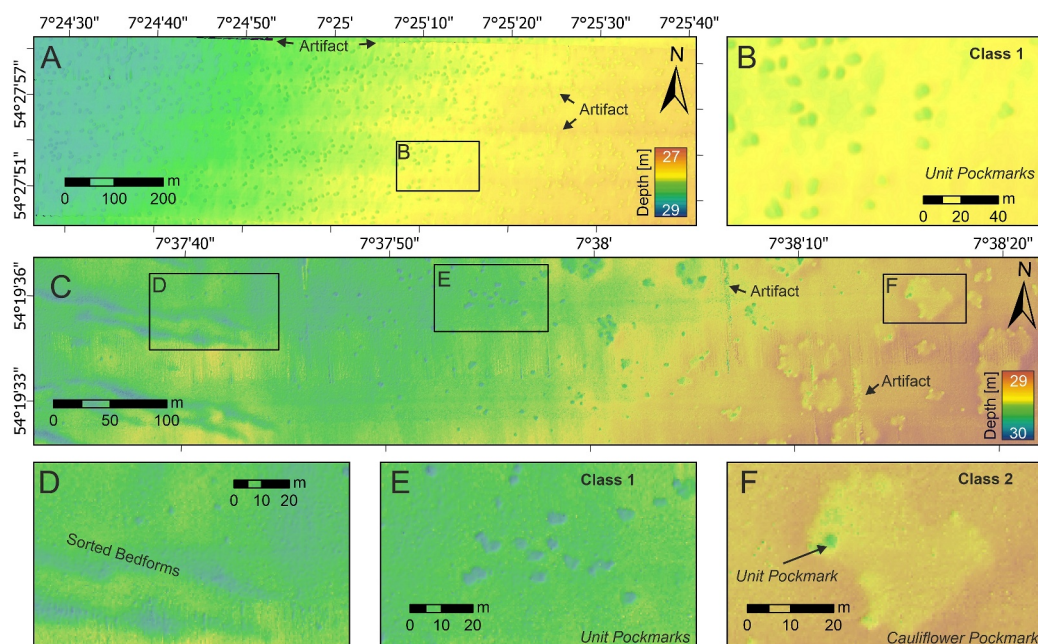


Figure 4. Bathymetric data showing the distinct types of pockmarks and bedforms in the survey area (location shown in Figure 1). (a) Bathymetric data showing the same survey area as surveyed by (Krämer et al., 2017) with large quantities of unit pockmarks (Class 1). Slight east-west banding is an artifact induced by an erroneous sound velocity profile creating a cross-track refraction effect (“frown”). (b) Zoom-In to (a) showing the unit pockmarks, which are solitary, small-scale, round depressions on the seafloor. (c) Bathymetric data south of the offshore windfarms (see Figure 1) with different classes of pockmarks and sorted bedforms. Along-track (East-West) middle latitudes show heave artifacts (“tractor marks”). (d) Zoom-in to elongated sorted bedforms that strike in 100–120° direction. (e) Zoom-In to unit pockmarks (Class 1) in panel (c). (f) Zoom-In to the complex-shaped pockmarks (class 2) also termed cauliflower pockmarks.

(Class 2, $N = 36,913$; Figure 5f). The pockmarks are not strictly circular and have a much larger perimeter than a circle with the same surface area, highlighting their complex shape. The separation of the two classes is reflected in the orientation of the minimum bounding geometry (as a parameter for pockmark orientation), which shows that class 1 pockmarks exhibit no preferential strike direction, while class 2 pockmarks show a clear trend toward 100–120° (Figure 5i). Orientation of pockmark shapes can be influenced by local and regional bottom currents. In the survey area, ocean currents rotate anticlockwise with speeds of up to 0.9 m/s (Figure 6). The highest ocean current speeds are oriented around 90–120° (Figure 6), correlating with the primary orientation of the pockmarks (Figure 5).

Apart from circularity, distributions of individual parameters show no clear distinction for each class, highlighting that pockmarks of all shapes exist in between the two end-member shapes (Figure 5c). Both classes of pockmarks show a very low relief (mean: 27 cm, median: 21 cm) with Class 2 pockmarks exhibiting a much higher areal extent while maintaining the same vertical relief (Figure 5). The water depth at which pockmarks occur also shows distinct clusters. A Bayesian-Gaussian-Mixture-Model produces three clusters of normal-distributed pockmarks (Figure 5). The three clusters are mapped around average water depth values of about 26, 29, and 32 m. These depth intervals are consistent across the entire data set and are unlikely to result from targeted sampling as all depth intervals from 20 to 45 m were surveyed. All three clusters show pockmarks of both classes.

Within the same three depth intervals where pockmarks cluster (26, 29 and 32 m), we find distinct elongated depressions on the seafloor, which we classify into two types based on their characteristics. The first type exhibits a complex morphology with no clear strike directions. These depressions show high backscatter at their deepest areas. However, while the northwestern edges of the high backscatter are sharp, the southeastern edges appear diffuse. The overall meandering morphology of these features resembles present-day tidal flats or channels (Figure 7a/7b). Pockmarks are visible in the vicinity but outside of these features. The second type comprises of elongated depressions (furrows), which have lengths of tens to hundreds of meters (Figure 7c/7d) and show a

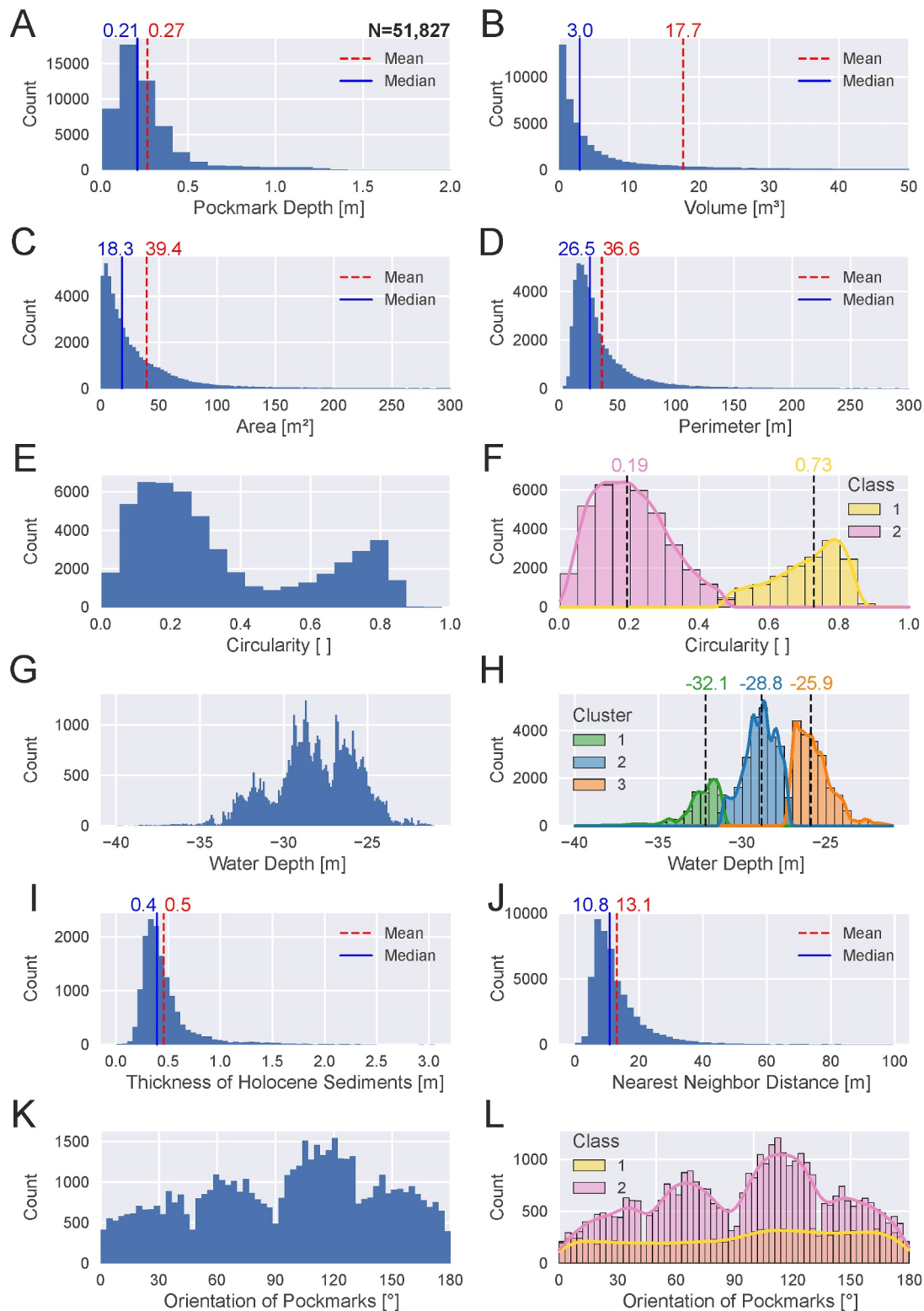


Figure 5. Statistical analyses of main geomorphological parameters including (a) pockmark depth, (b) pockmark volume, (c) area, (d) Perimeter, (e) Circularity (f) Circularity with Bayesian-Gaussian-Mixture model showing the two classes of pockmarks, (g) water depths of pockmarks, (h) water depths of pockmarks with Bayesian-Gaussian-Mixture model showing three clusters, (i) thickness of the topmost (Holocene) sedimentary layer, (j) nearest neighboring distance in between individual pockmarks, and (k) orientation of the minimum bounding geometry as a parameter for pockmark orientation, (l) orientation of pockmarks grouped by class (see f).

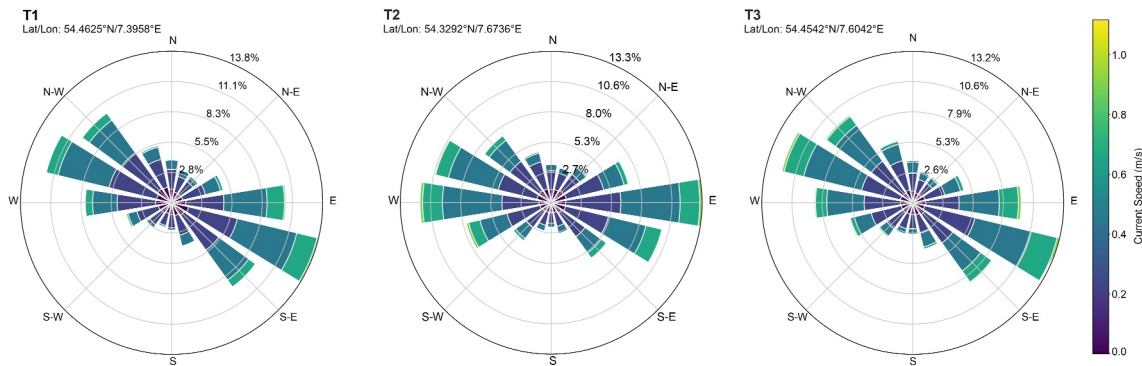


Figure 6. Rose diagram plots of ocean surface current velocity and direction in the survey area at three distinct locations during the year of cruise MSM99/2 (2021/01/01–2021/12/31). The concentric circles are annotated with percentage values representing the cumulative frequency of occurrences within that radius over the year. The strongest current directions are in East-West directions with a slight shift toward northwest to southeast. Locations of extracted data are shown in Figure 1.

distinct northwest-southeast strike direction (100° – 120°). These furrows show high backscatter while being separated by morphological ridges with low backscatter. There are no pockmarks in the vicinity of these features.

3.2. Parasound Data

In general, the top sediments can be characterized by a fine lamination of seismic reflections or completely transparent facies comprising almost no impedance contrasts. The topmost sediments are generally very thin in the survey area. Our data show that pockmarks predominantly occur in areas where the thickness of the topmost sedimentary layer is less than 1 m (avg. $0.5 \text{ m} \pm 0.25 \text{ m}$) but can occur up to 3 m sediment thickness. The topmost sediments are clearly separated from the unit below (Figure 8). The unit below shows a transparent to chaotic seismic facies. In multiple locations across the survey area, this boundary shows strong reflections or bright spots with dimming of amplitudes below (Figure 8). However, there are no visible seismic anomalies that connect these strong reflections with any deeper subsurface structures (i.e., seismic pipe or chimney structures connecting

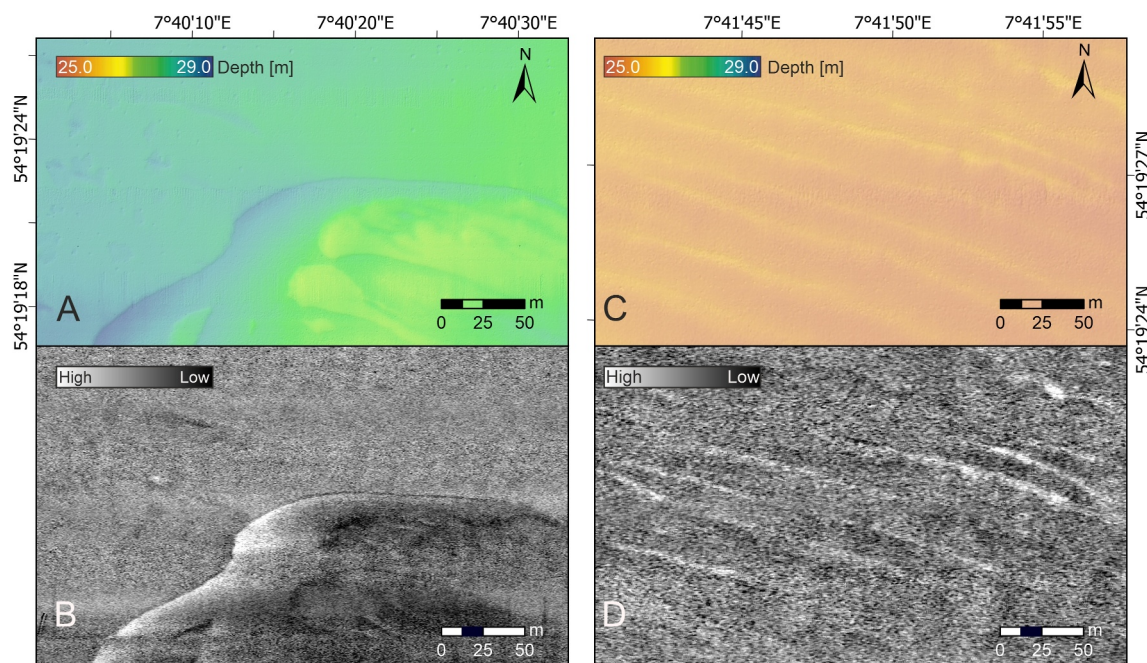


Figure 7. Bathymetric data from focus area 3 (location shown in Figure 1) showing depth and backscatter information. High backscatter is shown in white and low backscatter in black. (a) Depth map of complex ripple scour depressions that resemble present-day tidal flats or channels with (b) high backscatter inside the ripple scour depressions. (c) Depth map of the elongated ripple scour depression of 10 to hundreds of meters in length and (d) high backscatter within these depressions.

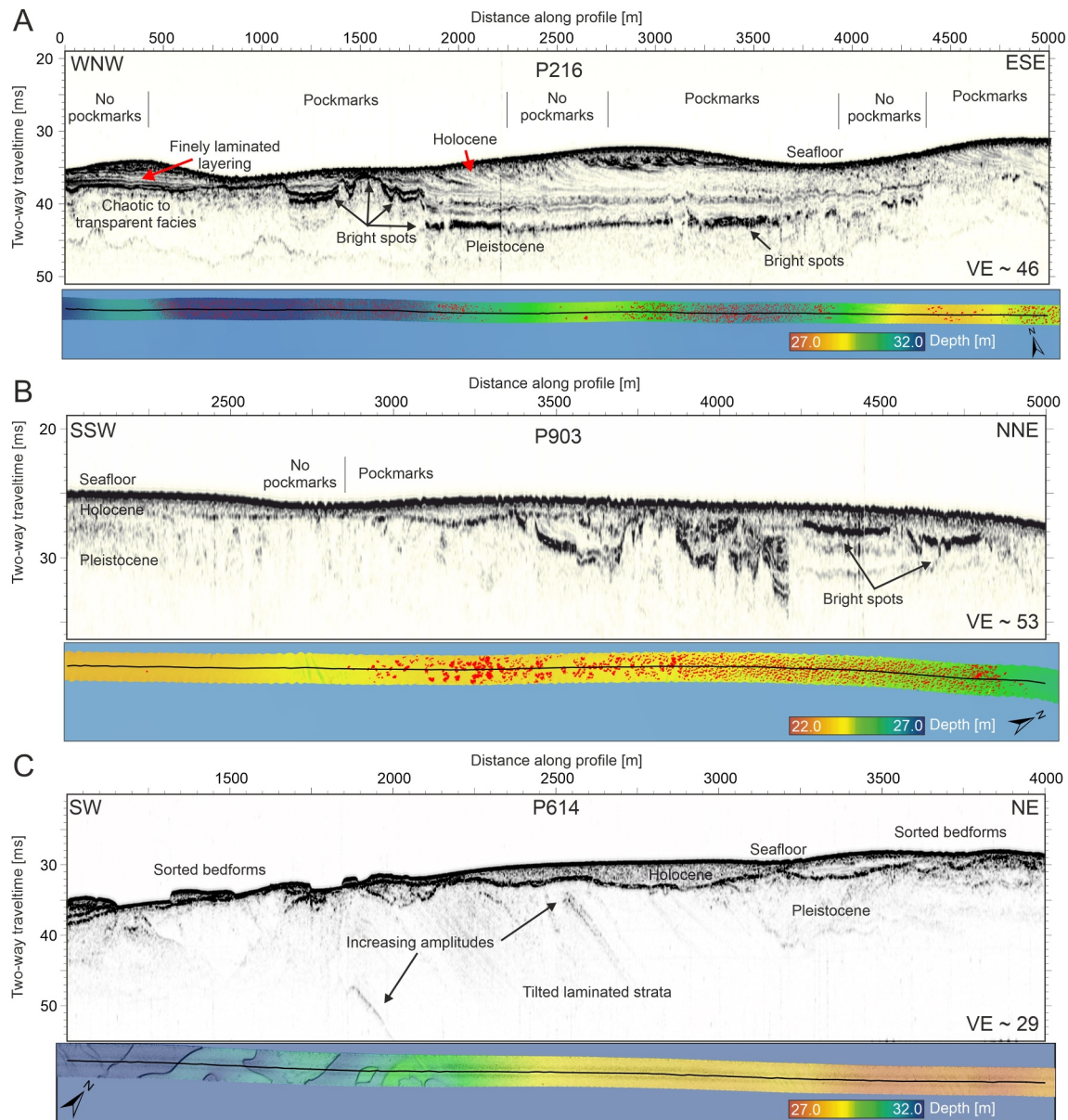


Figure 8. Parasound profiles across pockmark fields with map views of the exact profile tracks on our bathymetric data (with pockmarks outlined by red polygons). (a) 5 km-long profile P216 in northwestern part of the survey area. (b) 3 km-long profile P903 in the northeastern part of FA2. (c) 3 km-long profile P614 in the southwestern part of the survey area showing the influence of salt domes in the area on the sedimentary succession (tilted strata) and abundant sorted bedforms at the seafloor. Location of profiles shown in Figure 1.

deeper strata with the shallow stratigraphy). The clear separation of seismic facies likely represents the change from Holocene to Pleistocene sediments (Coughlan et al., 2018; Hoffmann et al., 2022; Krämer et al., 2017). The Pleistocene sediments show dipping reflections (Figure 8), which likely indicate the presence of numerous paleo-valleys and in some locations potentially even deeper situated tunnel valleys (c.f. Lohrberg et al., 2020).

Close to the salt domes, we observe steeply dipping (near-vertical) reflections of shallow sedimentary strata. However, while we can see the very steeply inclined sedimentary layers at the surface sediments, there is no indication of upward migration of fluids, no flares visible in the water column nor any correlation to pockmark occurrences. In addition, we did not observe any amplitude anomalies indicative of gas release into the water column above those dipping layers.

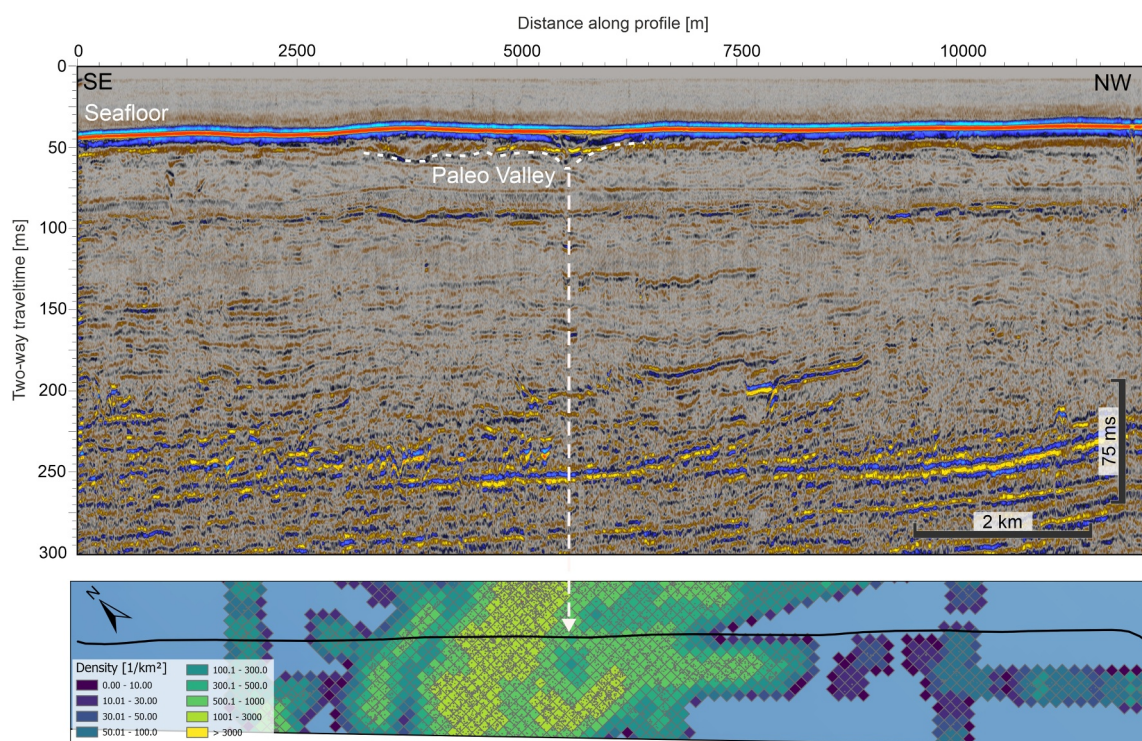


Figure 9. 12-km-long seismic profile P7007 across the northwestern survey area shows a paleo-valley that coincides with the pockmark field. The density of pockmarks per square kilometer does, however, not show good correlation with the paleo-valley. Location of profile shown in Figure 1.

3.3. Seismic Data

Our seismic data show no vertical seismic anomalies such as chimneys or pipes that would indicate a hydraulic connection between seafloor pockmarks and deeper strata. Below the seafloor, the data show infilled paleo-valleys, probably related to fluvial and/or glacial processes. The sparse data coverage hinders a clear determination of the drainage direction, but the mapping suggests that most valleys are oriented in an east-west or a southwest-northeast direction, which would match local paleo-drainage patterns related to paleo-rivers (east-west, Krämer et al., 2017) or related to tunnel-valleys (southwest-northeast, Lohrberg et al., 2020). Pockmark abundance, however, shows no positive correlation with valley distribution (Figure 9).

3.4. Geochemical Data

Geochemical porewater data from subsurface sediment samples (0–55 cm) were classified into three categories (Figure 10): (a) Sampled inside the pockmark (pink dots); (b) Sampled outside the pockmark (green dots); (c) The exact spot is not defined (gray and black dots). Four geochemical parameters indicative of porewater freshening (chloride), thermogenic/microbial gas migration and accumulation (i.e., methane), and shallow microbially induced diagenesis (alkalinity and sulfate) are illustrated in Figure 11.

Alkalinity increases from ~ 2.3 at the sediment surface to 8 meq L^{-1} at 45 cm sediment depth (Figure 10a). However, no difference between “inside” and “outside” alkalinity is indicated. The organic matter content, which probably fuels microbially induced diagenesis and related alkalinity increase, is characterized by its marine origin (C/N ratio: 8.2–10.5). The organic carbon content of, for example, GC25 (see Figure 1) is in the range of 0.3–0.5 wt.% and Ca-carbonate content is between 1.6 and 3.2 wt.%.

The measured chloride concentrations ranged between 500 and 550 mM with no significant difference between inside and outside (Figure 10b). No freshening trend with depth was indicated by the porewater data of GC25. The variability of calculated porewater salinity, based on chlorinity data of surface sediment chlorinity (32–35.2), is comparable to bottom water salinity variation of 31.5–33.8 measured during the MSM99/2 cruise.

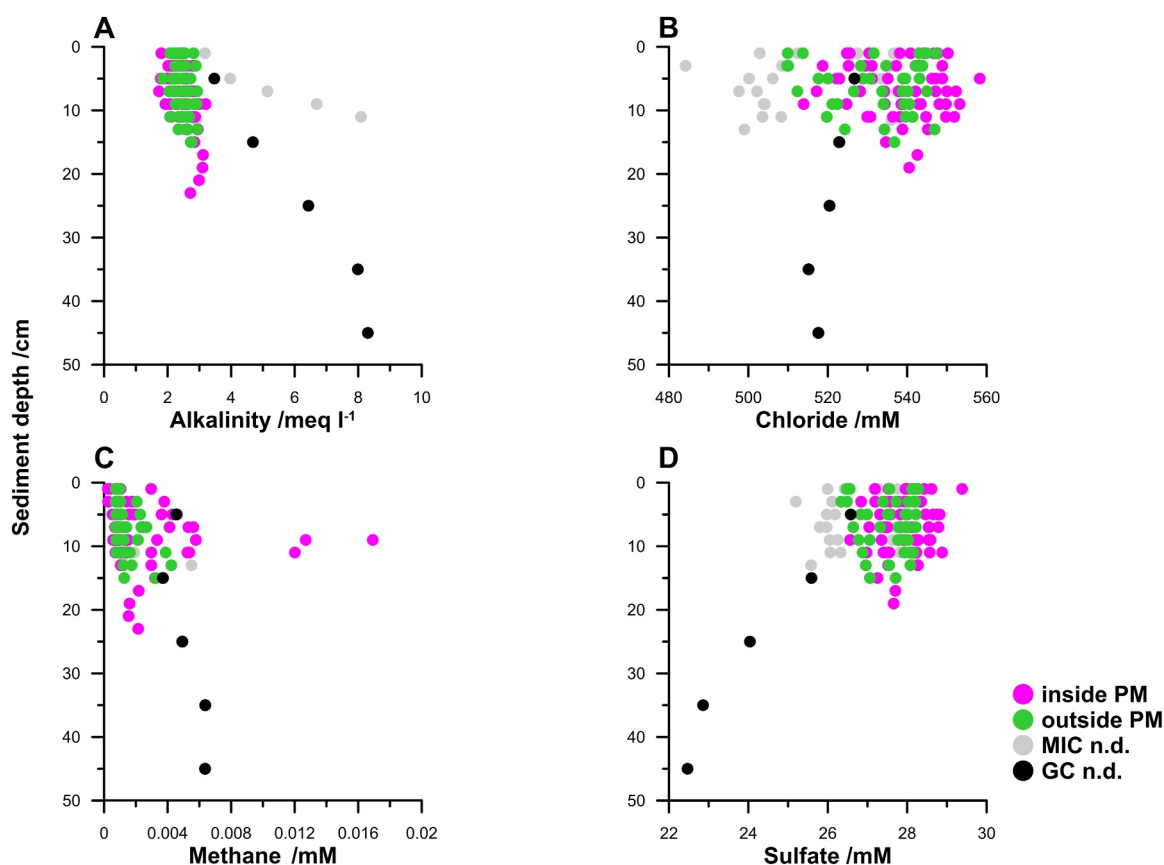


Figure 10. Selected geochemical porewater data of Mini-Multi Corer (MIC) and Gravity Corer (GC25) samples. The graphs show (a) Alkalinity, (b) Chloride, (c) Methane, and (d) Sulfate. Locations are shown in Figure 1.

Methane concentrations of wet sediment samples ranged in the same lower order of magnitude, that is, <0.02 mM in all classified categories (Figure 10c). However, the mean methane concentration (0.0025 mM, $n = 58$) from inside pockmarks is slightly higher compared to the outside pockmark mean value (0.001 mM, $n = 20$). The highest concentration of methane measured inside a pockmark is less than 0.02 mM though. This is only about 0.4% of a calculated methane oversaturation at 20–35 m water depths, water temperature of $\sim 5^{\circ}\text{C}$, and salinity of ~ 33 .

Neither a correlation of sulfate content with classified categories nor any significant sulfate concentration decrease is indicated in the porewater data of the MIC samples (Figure 10d). However, sulfate decrease in GC25 points toward a sulfate-methane transition zone at over 200 cm sediment depth.

Grain size analysis of the sediment samples in the survey area revealed that the topmost layer (0–20 cm) is dominated of well sorted fine to medium sand (Figure 11). Surface samples show strong bioturbation indications including in situ living mollusks and echinoidea, and shell debris as well. The macrozoobenthic community dominated by *Lanice conchilega* (Figure 11) resides on the seafloor. Shell debris at very shallow depths prohibited subsurface sampling within many pockmarks and further penetration of GCs as well as MICs.

4. Discussion

4.1. Morphology and Modification of Pockmarks

The modification of pockmarks by subsequent ocean current interaction and scouring is a common process described in various marine settings (Andresen et al., 2008; Andrews et al., 2010; Brothers et al., 2011; Fandel et al., 2017; Gafeira et al., 2012; Hillman et al., 2018, 2023; Micallef et al., 2022; Schattner et al., 2016). Pockmarks that are exposed to oceanographic currents over time develop an elongated shape, which is oriented in

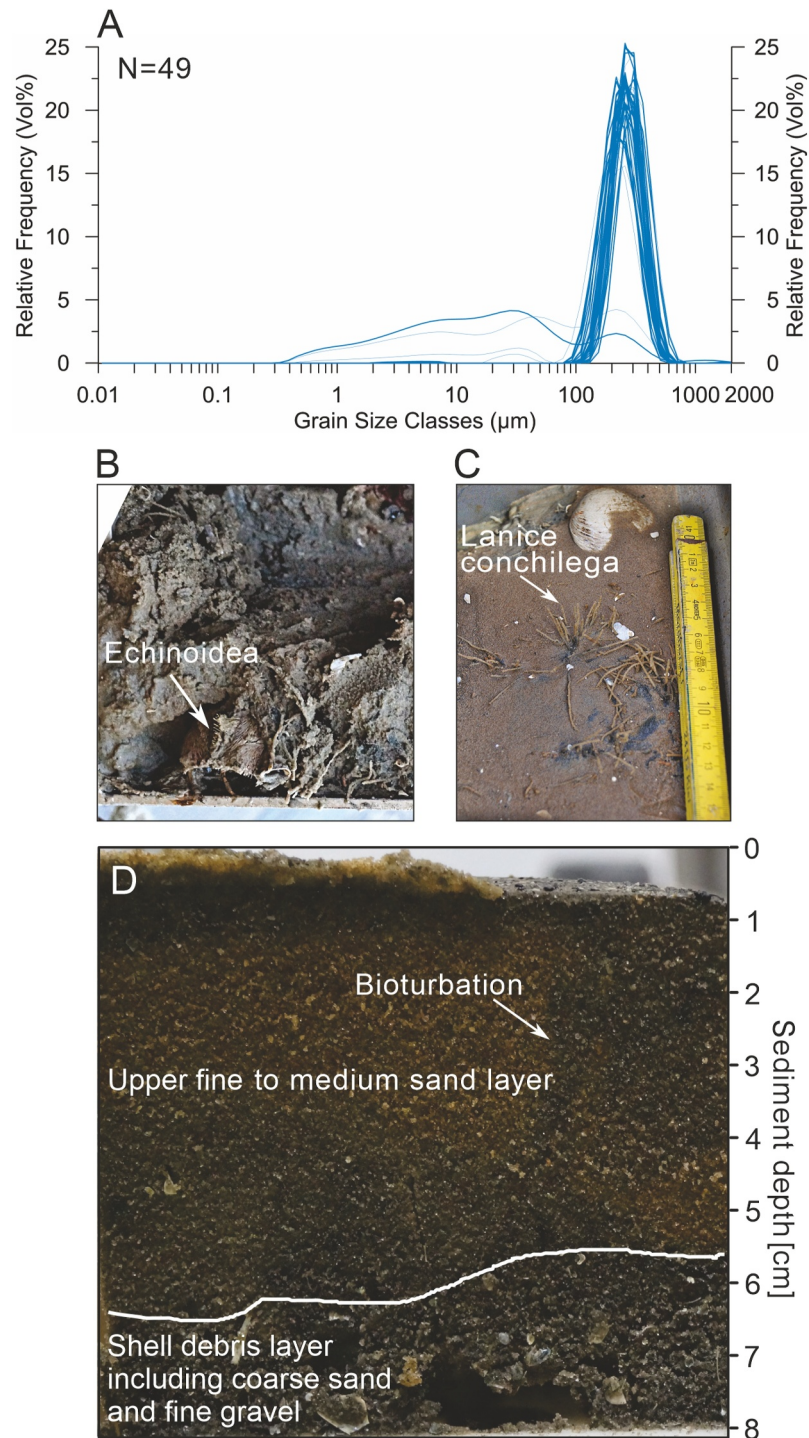


Figure 11. Sedimentological analyses of samples acquired during MSM99/2. (a) Grain size distribution of all surface samples (0–20 cm sediment depth) showing unimodal distribution with a mean value in medium sand. (b) Grab and MIC samples often include in situ living mollusks and echinoidea. (c) The sediment surface is often covered by special worms called *Lanice conchilega* that stabilize the sediment surface. (d) Bioturbations occur in all MIC and grab samples. Here, the coarse debris layer including coarse sand is at ~5 cm depth but is more often found at ~20 cm depth.

the direction of the primary ocean current. Indeed, our data show a slight elongation trend toward 90–120° in the pockmark orientation (Figures 5k and 5l). This orientation matches the high-backscatter elongated depressions (furrows) in our data set. We interpret these as rippled scour depressions (RSD), also called sorted bedforms,

which are discordant, elongated depressions with coarser grain sizes in their deeper situated areas (Cacchione et al., 1984; Murray & Thieler, 2004). The abundant occurrence of sorted bedforms indicates a strong resonance of the surficial sediments with the tides and storms (Diesing et al., 2006). The orientation of the elongated RSD is along the highest ocean current velocities (90–120°, see Figures 6 and 7). The collocation of RSDs in the same depth intervals as the pockmarks as well as their preferred orientation in the same direction (90–120°, Figure 5) indicate an oceanographic component in the modification but potentially also the formation of the pockmarks (see 4.4 Alternative Formation Mechanisms). Currents flowing across the pockmarks likely erode material or create enough turbulence to start feedback mechanisms by which finer material settling is inhibited inside the pockmarks with their coarse-grained base (Murray & Thieler, 2004). This process can be clearly seen from the analyses of the pockmark orientation grouped by the two classes: While initial pockmarks are round-shaped (Class 1, Figure 5I), reshaping of pockmarks by bottom currents creates a slight trend in pockmark orientation (100–120°, Figure 5I). However, pockmarks of all orientations exist throughout both classes suggesting a rather multidirectional growth with turning tides than a preferred elongation in only one direction (see Figure 3). This multidirectional growth also explains the complex cauliflower pockmarks.

In summary, our time lapse data suggests a distinct spatiotemporal evolution in four steps. The first step is the formation of initial depressions as (semi-) circular features of probably even less than 1 m in diameter (Figure 3, Class 1 in Figures 5f and 5I). In a second step, the features are subsequently modulated by secondary alteration related to strong ocean currents (Figure 6). While the rims of the pockmarks start to erode, the depth remains the same (Figures 5a and 5I). The depth-limit is likely limited by a shallow situated shell detritus layer (20–30 cm; Figure 11) or coarse-grained sediments of the Pleistocene (Coughlan et al., 2018), which also explains the high backscatter in multibeam data inside the pockmarks. The third step in evolution is the intermingling and coalescence of pockmarks until individual depressions cannot be recognized anymore and only the rims of previous pockmarks remain (c.f. Schneider von Deimling et al., 2023). During the fourth step, the pockmarks and remaining intermingled rims vanish completely and the seafloor returns to its flat and even shape (Figure 3). The seafloor reverts back to a sediment texture similar to what existed before the pockmarks emerged—fine to medium sands. This happens either over longer timescales (weeks, month) or during heavy storm events (hours, days), during which the whole sandy cover is dynamic (Hoffmann et al., 2022), and the seafloor gets leveled. Thus, the southeastern North Sea is a perfect location for sandy seafloor depressions to form and vanish.

4.2. Sand Versus Mud Pockmarks

Pockmarks in sand are, in contrast to muddy seafloors, largely underexplored in the world's oceans (Coleman et al., 2010; Jones et al., 2009; Judd & Hovland, 2009; Mueller, 2015; Scanlon et al., 2005; Szpak et al., 2015). Pockmarks associated with sand waves in fine- to medium grained carbonate ooze sands were discovered off the coast of Australia at water depths of 130 m (Jones et al., 2009). Industry data shows that the seafloor depressions newly form after the installation of seafloor infrastructure. As no time-lapse surveys exist, their lifespan on the seafloor remains unknown. Similar pockmark-like features in nearshore sandy environments may also form by scouring around mine-like objects on the sea floor and vanish over time (Jenkins et al., 2007; Mayer et al., 2007; Wilkens & Richardson, 2007). Later studies in the same region (Mueller, 2015) attributed similar pockmarks in carbonate sands to a biotic origin. Further, Scanlon et al. (2005) report on pockmarks created by red grouper in sandy carbonate environments in the Gulf of Mexico. Here, the red grouper continuously excavates pockmarks, which also vanish quickly if not maintained (Coleman et al., 2010). In the Dunmanus Bay, SW Ireland, Szpak et al. (2015) documented over one hundred pockmarks with small diameters (5–17 m) in sandy sediments that do not exceed 1 m in depth. They have linked these pockmarks to mild periodic venting of hydrocarbons. None of these reported sandy pockmarks show the very low depths with substantial extent (area) that we find in the southeastern North Sea.

We suggest this exceptional morphology results from the interplay between the sandy surface sediments and ocean current modification of the pockmarks. Although the initially small pockmarks (Class 1) we observe seem to have a similar depth to perimeter relationship to most other pockmarks (Figure 12), the ocean current altered pockmarks (cauliflower pockmarks) do not show evidence of eroding deeper into the sediment than ~30 cm. While the constant movement of the medium sand at the seafloor interface by the strong bottom currents causes the pockmarks to form and vanish over time, their depth is essentially limited by the shallow situated shell detritus

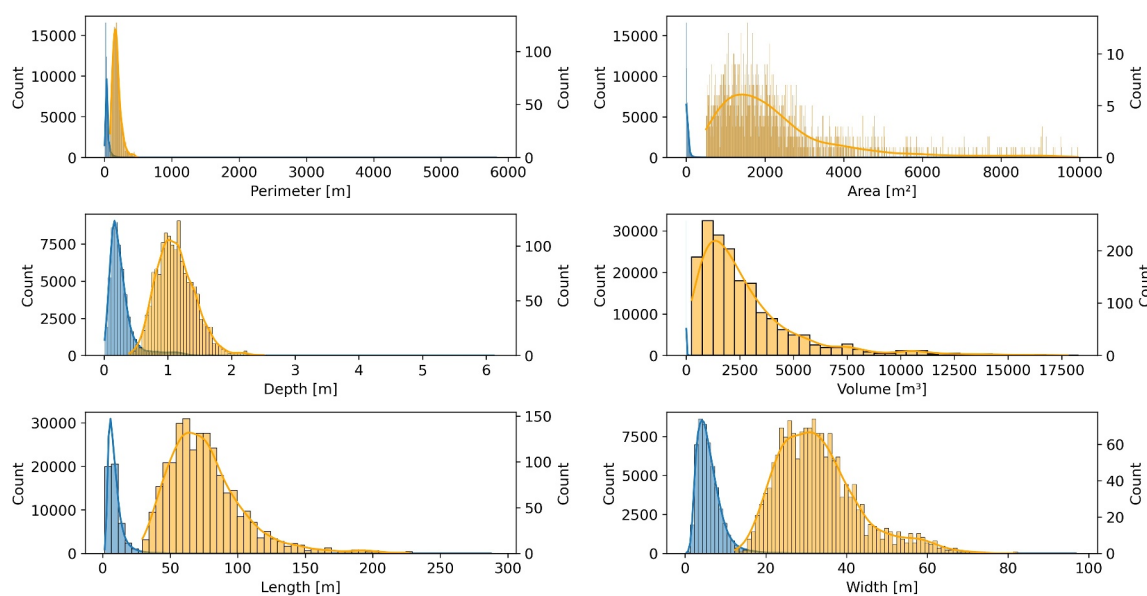


Figure 12. Comparison of main geomorphological parameters between pockmarks in the Scanner pockmark area (orange) and the pockmarks in the southeastern North Sea (blue). Both pockmarks are distinct from another which we correlate to the local lithology and corresponding geotechnical differences.

and coarse-grained sediments of the Pleistocene. While finer sediment is eroded and transported, the remaining shell fragments and larger grains reach a critical amount and inhibit further depth erosion.

The pockmarks described here form and vanish over the timespans of hours, days, and weeks rather than millennia. Small and short lasting depressions of 10s of cm depth have also been reported from Gullfaks field and Tommeliten site (Judd & Hovland, 2009). Their shallow incision depth (~30 cm) requires the improved capabilities of modern multibeam systems and higher repetition rates in reconnaissance surveys. We therefore suggest that pockmarks in sand are much more common than previously assumed and that the lack of case studies results from the lower preservation potential rather than less fluid migration or activity in sandy regions, similar to the preservation time of trawl marks on the seafloor (Brunns et al., 2020). Additionally, the discovery of these often shallow, small, and short-lasting depressions is technically challenging.

In conclusion, silty to muddy lithologies seem to enable the formation of pockmarks that are very long-lived structures, hard to remobilize and usually get reshaped marginally by collapse of oversteepened flanks or bottom currents. In contrast, our data suggests that pockmarks in sandy formations tend to be short-lived, barely visible structures that can form in highly mobile sands, which makes them form and vanish fast over short timescales.

4.3. Seafloor Fluid Seepage as Formation Mechanism

Pockmarks in the southeastern North Sea develop in sandy sediments with exceptional low depth despite the large areas they cover. The question remains, why do these pockmarks initially form? The formation of pockmarks is usually linked to hydrocarbons, which are advected from deep (thermogenic) or shallow (biogenic) sources (Judd & Hovland, 2009). Our data show no hydraulic connection between pockmarks and deeper strata. The seismic data do not reveal any vertical seismic anomalies crosscutting strata, no correlation of pockmarks with the salt diapirs and the geochemical data do not indicate any recent methane accumulation in surface sediment or gas release into the water column during MSM99-2. Thus, we exclude a deeper (thermogenic) gas source to be responsible for pockmark formation.

Krämer et al. (2017) proposed a formation mechanism for the pockmarks in the southeastern North Sea by which pressure relief under a passing wave triggers the expulsion of shallow (biogenic) methane. The abrupt release of methane potentially leaves an initial depression at the seafloor, which is further scoured by strong tidal currents to form the pockmarks over time. However, the measured dissolved methane concentrations in the subsurface are

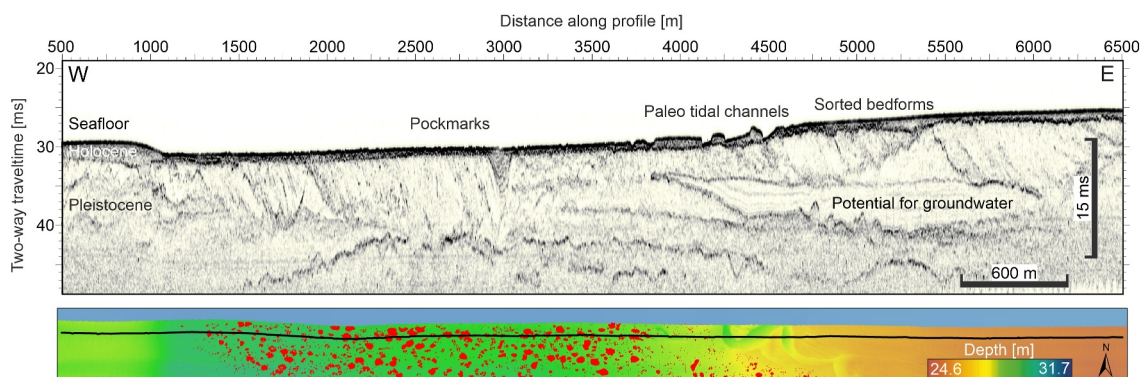


Figure 13. Top: 6-km-long Parasound profile with automatic gain control on amplitudes crossing the pockmarks from West to East within FA3. Holocene sediments are clearly separated from Pleistocene and possible Neogene sediments. Potential groundwater-bearing units are indicated. At the surface, paleo-tidal channels cut deep (>1 m) into the sedimentary succession, while they are clearly separated from the adjacent sorted bedforms by their morphology. Pockmarks are outlined by red polygons.

very low (Figure 10). The subsurface data also show very few indications of shallow free gas (strong reflections, bright spots) at the Holocene/Pleistocene boundary (Figure 8). This shallow gas is potentially linked to paleo-peat submerged beneath the North Sea (Borges et al., 2016; Coughlan et al., 2018; Lippmann et al., 2021), shallow gas-bearing incised channels (Ahlrichs et al., 2024), or paleo-tidal flats (Engelen & Cypionka, 2009), which contain sufficient organic material to produce methane. The co-location of pockmarks and the complex sorted bedforms (potential paleo-tidal flat; Figure 7a/7b) within the same depth intervals (Figure 5f) suggests a genetic link. However, since bright spots are only observed in limited areas and given the very large number of pockmarks, it seems unlikely that they are the main driver behind pockmark formation.

In contrast to the theory of shallow gas activation by wave activity proposed by Krämer et al. (2017), Gupta et al. (2022) used numerical simulations to show that wave-induced pressure changes were dampened by free gas pockets and mobilization of the gas would not be possible. They showed that wave-induced pressure changes can lead to accumulation of free gas in the shallow subsurface as the phase transition of dissolved to free gas is strongly pressure dependent. However, this accumulation of free gas heavily relies on a pre-existing gas saturation in porewaters of minimum 50% (Gupta et al., 2022). Our data shows that the concentrations of methane are below 0.4% of in situ methane saturation and that there is no physical sealing barrier keeping dissolved methane from simply migrating into the water column. Moreover, microbial oxidation of methane would efficiently prevail any methane accumulation to reach oversaturation in the upper 2 m of sediment. Thus, this process can also not explain the formation of pockmarks by hydrocarbon ebullition.

The storm hypothesis evokes pressure changes in the subsurface as a main driver of pockmark formation. Our data show that the upper 20 cm to a few meters mainly consist of fine sand (Figure 11). These sands are highly mobile during storm events and tides (Hoffmann et al., 2022) and thus small depressions on the seafloor will likely be leveled during storm events. This is also supported by our time-lapse data set, where we find pockmarks in May and November 2021, which were likely leveled out by winter storm events when we resurveyed the area in February (Figure 3). This also explains the fast formation and disappearance of pockmarks. Our data thus suggest that pockmarks are leveled rather than formed during storm events, which is not in agreement with the hypothesis that pockmarks are formed during storm events (Gupta et al., 2022; Krämer et al., 2017). Furthermore, Krämer et al. (2017) suggested that a total release of 5,000 t of methane per year would be necessary to create the pockmarks. Considering the thousands of additional pockmarks observed since then, this amount would likely at least double. Our new geochemical and hydroacoustic data show that the expulsion of this large amount of methane should be considered unrealistic.

Pockmarks may also be formed by the continuous release of groundwater (Andresen et al., 2021; Hoffmann et al., 2023). Groundwater bearing glacial tunnel valleys with remnant/buried water bodies, infilled paleo riverbeds, or tidal channels with potential onshore links may provide the necessary source for freshwater (e.g., Figure 13). However, our data show no chloride depletion or any other geochemical anomaly in the survey area indicating groundwater seepage. It remains unclear how well-connected aquifers are and how vertical

groundwater seepage would be initiated. The coast is low lying and provides practically no or very little hydraulic head, which makes seepage this far offshore highly unlikely.

However, the absence of fluids during our campaign does not necessarily imply that fluids have not caused the pockmarks. The timing of sampling in relation to the yearly “life-cycle” of the pockmarks might be critical in identifying the involved fluids. Assuming that the pockmarks were initially formed rather quickly and then are left dormant until leveling by storms would imply that timing of sampling is very critical for documenting potential fluid flow. However, given the vast number of pockmarks that continuously form throughout the year, we would expect the measured values for chloride or methane to be well above the background. However, since gas concentrations in the sediment are minimal and no geochemical indications for freshened groundwater exist (Figures 10 and 13), we suggest that it is unlikely that large quantities of groundwater or methane are actively seeping to the seafloor. Our new findings imply that the substantial number of methane emissions (5,000 t (CH₄) yr⁻¹) that were previously proposed (c.f. Krämer et al., 2017) lack directly observable evidence and should be omitted or used with caution in future regional methane budgets. We thus conclude from our data that the ebullition of light hydrocarbons or groundwater is unlikely to have caused pockmark formation.

4.4. Alternative Formation Mechanisms

Schneider von Deimling et al. (2023) propose that vertebrates may cause the depressions and term them pits. The authors suggest that harbor porpoise feed on buried sandeels in an erosive manner, thus forming pits in the sandy seafloor, which serve as nuclei for scouring. Such pits were first reported to be formed by gray whales (Johnson & Nelson, 1984) and later addressed to be caused by other whales, fish, or other benthic biota. For example, a study from the Australian continental shelf proposed that pockmark-like structures of significant size might be formed by fish (Mueller, 2015). The yellowed grouper (*Epinephelus flavolimbatus*) is known to excavate large trenches and burrows that are several meters wide and can reach up to 1.5 m depth (Jones et al., 2009). In 2022, a research cruise to the Weddell Sea found 60 million nests of Antarctic icefish over 240 square kilometers. The nests resemble pockmarks with ~75 cm diameter, ~15 cm depth and a very dense spacing of ~25 cm (Purser et al., 2022). All these pockmark-like bio-structures are characterized by a very shallow incision depth. This is in line with our data showing a very shallow incision depth (~30 cm), a close spacing (~13 m) and low volume ~ 3 m³.

For the southeastern North Sea, there are good indications for the harbor porpoise theory as the pits are formed close to the tidal mixing front, occur in sand eel habitats, and are characterized by shallow incision depth independent of the perimeter (Schneider von Deimling et al., 2023). Given the large number of porpoises predicted to inhabit our survey area (Gilles et al., 2016), porpoise feeding could explain the large abundance (>50,000) of pockmarks we found. In combination with the tidal current scouring of the initial depressions, this could explain the formation of pockmark-like structures similar to the proposed mechanism for pockmark formation by Krämer et al. (2017).

An oceanographic component in the modification is evident from our data, but potentially also the formation of the pockmarks can be initiated by hydrodynamic processes. The formation of short-lived pockmarks by strong orbital waves during growth and decay of storms has been shown in nearshore observations (Speller, 2000). Hence, coarser grained material (here *Lanice conchilega*, shell detritus or the Pleistocene sediments) could act as nuclei for complex scouring (Venditti et al., 2005). This process could also explain the large abundance of pockmarks in the survey area, the formation and disappearance as well as the absence of any fluid indications. This process, however, has only been described for a nearshore environment. Continuous observations through moored instruments or fiber optic cables across multiple disciplines (e.g., oceanography, biology, geology) could help to further constrain the responsible formation mechanism.

5. Conclusions

We analyzed over 50,000 pockmarks to understand their morphological characteristics and define a new class of pockmarks. These sandy pockmarks form over short time periods in four distinct steps. They are different from other pockmarks in the North Sea by almost every geomorphological parameter we have measured. The main reason is likely the interplay between the highly mobile fine sand at the seafloor interface, the limiting shell detritus at shallow depth and intense scouring of the strong bottom currents. This combination provides an excellent environment to create and flatten out (form and vanish) pockmarks over short time periods. These

settings are, however, not unique to the North Sea and we expect similar pockmarks to occur in other tide-dominated shallow shelf settings around the world.

Pockmark formation is usually linked to the expulsion of fluids. However, our data show no signs of fluid ebullition. In the absence of evidence for hydrocarbon seepage, we also consider groundwater to drive pockmark formation. The potential for groundwater bearing geological units is high in this part of the North Sea as many buried fluvial channels and glacial tunnel valleys are present. However, we interpret that there is no evidence from our geochemistry data to support active groundwater seepage. Thus, neither the expulsion of hydrocarbons nor groundwater are the main drivers behind pockmark formation in the southeastern North Sea. Considering this lack of evidence for fluid seepage, we discuss benthic processes such as the hunting for prey by vertebrates as feasible mechanisms or solely oceanographic formation by complex ocean bottom current scouring. All the above-mentioned mechanisms rely on heavy scouring of the seafloor after an initial depression has been imprinted on the seafloor. While we cannot fully constrain the responsible mechanism for pockmark formation, we recommend further, possibly permanently installed research infrastructure that enables continuous or short interval monitoring at higher resolution with wider range acquisition methods (e.g., cameras and acoustic scanner). Such a monitoring strategy could be integrated into the existing FINO Research Platform in the North Sea (www.fino3.de).

Data Availability Statement

All data including geophysical, sedimentological, geochemical porewater and oceanographic data in the study are available at Pangaea Data Repository with CC-BY-4.0 (Schmidt et al., 2021). Data from the circulation model “BSH-HBMnoku” (surface elevation, ocean current speed and direction) (Bundesamt für Seeschifffahrt und Hydrographie, 2024) can be requested from the Federal Maritime and Hydrographic Agency (BSH).

Acknowledgments

We thank the captains, crews, and shipboard scientific parties of R/V Maria S. Merian Cruise MSM99/2 as well as R/V Heincke Cruises HE576, HE588, HE592, HE602. We thank two anonymous reviewers and the editor for a constructive review process which improved the manuscript substantially. We are thankful to the academic licensing programs of IHS for providing the Kingdom Seismic Interpretation Software, ESRI for providing the ArcGIS/Pro Software, Schlumberger for providing VISTA Seismic Processing Software and QPS for providing Qimera Software. We acknowledge financial support by the German Research foundation (GPF 21-1_013, Deutsche Forschungsgemeinschaft, DFG). Co-funded by the European Union under Grant 101060851. Open Access funding enabled and organized by Projekt DEAL.

References

- Ahrlrichs, N., Ehrhardt, A., Schnabel, M., & Berndt, C. (2024). Vertical acoustic blanking in seismic data from the German North Sea: A spotlight to shallow gas-bearing incised channels. *Journal of Quaternary Science*, 39(3), 421–431. <https://doi.org/10.1002/jqs.3590>
- Andresen, K. J., Dahlin, A., Kjeldsen, K. U., Roy, H., Bennike, O., Norgaard-Pedersen, N., & Seidenkrantz, M. S. (2021). The longevity of pockmarks - A case study from a shallow water body in northern Denmark. *Marine Geology*, 434, 106440. <https://doi.org/10.1016/j.margeo.2021.106440>
- Andresen, K. J., Huuse, M., & Clausen, O. R. (2008). Morphology and distribution of Oligocene and Miocene pockmarks in the Danish North Sea - Implications for bottom current activity and fluid migration. *Basin Research*, 20(3), 445–466. <https://doi.org/10.1111/j.1365-2117.2008.00362.x>
- Andrews, B. D., Brothers, L. L., & Barnhardt, W. A. (2010). Automated feature extraction and spatial organization of seafloor pockmarks, Belfast Bay, Maine, USA. *Geomorphology*, 124(1–2), 55–64. <https://doi.org/10.1016/j.geomorph.2010.08.009>
- Baird, T. A. (1988). Female and male territoriality and mating system of the sand tilefish, *Malacanthus plumieri*. *Environmental Biology of Fishes*, 22(2), 101–116. <https://doi.org/10.1007/bf00001541>
- Borges, A. V., Champenois, W., Gypens, N., Delille, B., & Harlay, J. (2016). Massive marine methane emissions from near-shore shallow coastal areas. *Scientific Reports-Uk*, 6(1), 27908. <https://doi.org/10.1038/srep27908>
- Böttner, C., Berndt, C., Reinardy, B. T., Geersen, J., Karstens, J., Bull, J. M., et al. (2019). Pockmarks in the Witch Ground Basin, Central North Sea. *Geochemistry, Geophysics, Geosystems*, 20(4), 1698–1719. <https://doi.org/10.1029/2018gc008068>
- Böttner, C., Haeckel, M., Schmidt, M., Berndt, C., Vielstädte, L., Kutsch, J. A., et al. (2020). Greenhouse gas emissions from marine decommissioned hydrocarbon wells: Leakage detection, monitoring and mitigation strategies. *International Journal of Greenhouse Gas*, 100, 103119. <https://doi.org/10.1016/j.ijggc.2020.103119>
- Brothers, L. L., Kelley, J. T., Belknap, D. F., Barnhardt, W. A., Andrews, B. D., & Maynard, M. L. (2011). More than a century of bathymetric observations and present-day shallow sediment characterization in Belfast Bay, Maine, USA: Implications for pockmark field longevity. *Geological Marine Letters*, 31(4), 237–248. <https://doi.org/10.1007/s00367-011-0228-0>
- Bruns, I., Holler, P., Capperucci, R. M., Papenmeier, S., & Bartholomä, A. (2020). Identifying Trawl Marks in North Sea Sediments. *Geosciences*, 10(11), 422. <https://doi.org/10.3390/geosciences10110422>
- Bundesamt für Seeschifffahrt, & Hydrographie, B. (2024). BSH-HBMnoku. In *Hydrodynamik*. opmod@bsh.de.
- Bussmann, I., Damm, E., Schlüter, M., & Wessels, M. (2013). Fate of methane bubbles released by pockmarks in Lake Constance. *Biogeochemistry*, 112(1–3), 613–623. <https://doi.org/10.1007/s10533-012-9752-x>
- Cacchione, D. A., Drake, D. E., Grant, W. D., & Tate, G. B. (1984). Rippled scour depressions on the inner continental-shelf off central California. *Journal of Sedimentary Petrology*, 54(4), 1280–1291.
- Chenrai, P., & Huuse, M. (2017). Pockmark formation by porewater expulsion during rapid progradation in the offshore Taranaki Basin, New Zealand. *Marine and Petroleum Geology*, 82, 399–413. <https://doi.org/10.1016/j.marpetgeo.2017.02.017>
- Coleman, F. C., Koenig, C. C., Scanlon, K. M., Heppell, S., Heppell, S., & Miller, M. W. (2010). Benthic habitat modification through excavation by red grouper, *Epinephelus morio*, in the northeastern Gulf of Mexico. *The Open Fish Science Journal*, 3(1), 1–15. <https://doi.org/10.2174/1874401x01003010001>
- Coughlan, M., Fleischer, M., Wheeler, A. J., Hepp, D. A., Hebbeln, D., & Mörz, T. (2018). A revised stratigraphical framework for the Quaternary deposits of the German North Sea sector: A geological-geotechnical approach. *Boreas*, 47(1), 80–105. <https://doi.org/10.1111/bor.12253>
- Davy, B., Pecher, I., Wood, R., Carter, L., & Gohl, K. (2010). Gas escape features off New Zealand: Evidence of massive release of methane from hydrates. *Geophysical Research Letters*, 37(21). <https://doi.org/10.1029/2010gl045184>

- Diesing, M., Kubicki, A., Winter, C., & Schwarzer, K. (2006). Decadal scale stability of sorted bedforms, German Bight, southeastern North Sea. *Continental Shelf Research*, 26(8), 902–916. <https://doi.org/10.1016/j.csr.2006.02.009>
- Dimitrov, L., & Woodside, J. (2003). Deep sea pockmark environments in the eastern Mediterranean. *Marine Geology*, 195(1–4), 263–276. [https://doi.org/10.1016/s0025-3227\(02\)00692-8](https://doi.org/10.1016/s0025-3227(02)00692-8)
- Dumke, I., Berndt, C., Crutchley, G. J., Krause, S., Liebetrau, V., Gay, A., & Couillard, M. (2014). Seal bypass at the Giant Gjallar Vent (Norwegian Sea): Indications for a new phase of fluid venting at a 56-Ma-old fluid migration system. *Marine Geology*, 351, 38–52. <https://doi.org/10.1016/j.margeo.2014.03.006>
- Engelen, B., & Cypionka, H. (2009). The subsurface of tidal-flat sediments as a model for the deep biosphere. *Ocean Dynamics*, 59(2), 385–391. <https://doi.org/10.1007/s10236-008-0166-1>
- Fandel, C. L., Lippmann, T. C., Irish, J. D., & Brothers, L. L. (2017). Observations of pockmark flow structure in Belfast Bay, Maine, Part 1: Current-induced mixing. *Geo-Marine Letters*, 37(1), 1–14. <https://doi.org/10.1007/s00367-016-0472-4>
- Feldens, P., Schmidt, M., Mücke, I., Augustin, N., Al-Farawati, R., Orif, M., & Faber, E. (2016). Expelled subsalt fluids form a pockmark field in the eastern Red Sea. *Geo-Marine Letters*, 36(5), 339–352. <https://doi.org/10.1007/s00367-016-0451-9>
- Gafeira, J., Long, D., & Diaz-Doce, D. (2012). Semi-automated characterisation of seabed pockmarks in the central North Sea. *Near Surface Geophysics*, 10(4), 303–315. <https://doi.org/10.3997/1873-0604.2012018>
- Gilles, A., Viquerat, S., Becker, E. A., Forney, K. A., Geelhoed, S. C. V., Haelters, J., et al. (2016). Seasonal habitat-based density models for a marine top predator, the harbor porpoise, in a dynamic environment. *Ecosphere*, 7(6). <https://doi.org/10.1002/ecs2.1367>
- Grasshoff, K., Kremling, K., & Ehrhardt, M. (2009). *Methods of seawater analysis*. John Wiley & Sons.
- Gupta, S., Schmidt, C., Böttner, C., Rüpke, L., & Hartz, E. H. (2022). Spontaneously exsolved free gas during major storms as an ephemeral gas source for pockmark formation. *Geochemistry, Geophysics, Geosystems*, 23(8). <https://doi.org/10.1029/2021gc010289>
- Hein, F. J., & Syvitski, J. P. M. (1989). Sea-floor Gouges and pits in deep Fjords, Baffin-Island - Possible Mammalian feeding traces. *Geo-Marine Letters*, 9(2), 91–94. <https://doi.org/10.1007/bf02430429>
- Hillman, J. I. T., Klaucke, I., Pecher, I. A., Gorman, A. R., von Deimling, J. S., & Bialas, J. (2018). The influence of submarine currents associated with the Subtropical Front upon seafloor depression morphologies on the eastern passive margin of South Island, New Zealand. *New Zealand Journal of Geology and Geophysics*, 61(1), 112–125. <https://doi.org/10.1080/00288306.2018.1434801>
- Hillman, J. I. T., Watson, S. J., Maier, K. L., Hoffmann, J. J. L., Bland, K. J., Warnke, F., et al. (2023). The diverse morphology of pockmarks around Aotearoa New Zealand. *Frontiers in Marine Science*, 10. <https://doi.org/10.3389/fmars.2023.1235928>
- Hoffman, J. J. L., Gorman, A. R., & Crutchley, G. J. (2019). Seismic evidence for repeated vertical fluid flow through polygonally faulted strata in the Canterbury Basin, New Zealand. *Marine and Petroleum Geology*, 109, 317–329.
- Hoffmann, J. J. L., Michaelis, R., Mielck, F., Bartholomä, A., & Sander, L. (2022). Multiannual seafloor dynamics around a subtidal rocky reef habitat in the North Sea. *Remote Sens-Basel*, 14(9), 2069. <https://doi.org/10.3390/rs14092069>
- Hoffmann, J. J. L., Mountjoy, J. J., Spain, E., Gall, M., Tait, L. W., Ladroit, Y., & Micallef, A. (2023). Fresh submarine groundwater discharge offshore Wellington (New Zealand): Hydroacoustic characteristics and its influence on seafloor geomorphology. *Frontiers in Marine Science*, 10. <https://doi.org/10.3389/fmars.2023.1204182>
- Hoffmann, J. J. L., von Deimling, J. S., Schröder, J. F., Schmidt, M., Held, P., Crutchley, G. J., et al. (2020). Complex eyed pockmarks and submarine groundwater discharge revealed by acoustic data and sediment cores in Eckernförde Bay, SW Baltic Sea. *Geochemistry, Geophysics, Geosystems*, 21(4). <https://doi.org/10.1029/2019gc008825>
- Hovland, M., Gardner, J. V., & Judd, A. G. (2002). The significance of pockmarks to understanding fluid flow processes and geohazards. *Geofluids*, 2(2), 127–136. <https://doi.org/10.1046/j.1468-8123.2002.00028.x>
- Jenkins, S. A., Inman, D. L., Richardson, M. D., Wever, T. F., & Wasyl, J. (2007). Scour and burial mechanics of objects in the nearshore. *IEEE Journal of Oceanic Engineering*, 32(1), 78–90. <https://doi.org/10.1109/joe.2007.890946>
- Johnson, K. R., & Nelson, C. H. (1984). Side-scan sonar assessment of gray whale feeding in the Bering Sea. *Science*, 225(4667), 1150–1152. <https://doi.org/10.1126/science.225.4667.1150>
- Jones, A. T., Kennard, J. M., Logan, G. A., Grosjean, E., & Marshall, J. (2009). Fluid expulsion features associated with sand waves on Australia's central North West Shelf. *Geo-Marine Letters*, 29(4), 233–248. <https://doi.org/10.1007/s00367-009-0137-7>
- Judd, A., & Hovland, M. (2009). *Seabed fluid flow: The impact on geology, biology and the marine environment*. Cambridge University Press.
- Karstens, J., Schneider von Deimling, J., Böttner, C., Elgert, J., Hilbert, H.-S., Kühnt, M., et al. (2018). RV ALKOR Cruise Report 512 [AL512]-North Sea Blowouts. 15th July-26th July, 2018, Cuxhaven-Kiel (Germany).
- Karstens, J., Schneider von Deimling, J., Berndt, C., Böttner, C., Kühn, M., Reinardy, B. T. I., et al. (2022). Formation of the Figge Maar Seafloor Crater during the 1964 B1 Blowout in the German North Sea. *Earth Science, Systems and Society*, 2. <https://doi.org/10.3389/esss.2022.10053>
- Kelley, J. T., Dickson, S. M., Belknap, D. F., Barnhardt, W. A., & Henderson, M. (1994). Giant sea-bed pockmarks - Evidence for gas escape from Belfast Bay, Maine. *Geology*, 22(1), 59–62. [https://doi.org/10.1130/0091-7613\(1994\)022<0059:gsbpef>2.3.co;2](https://doi.org/10.1130/0091-7613(1994)022<0059:gsbpef>2.3.co;2)
- King, L. H., & MacLean, B. (1970). Pockmarks on the Scotian shelf. *Geological Society of America Bulletin*, 81(10), 3141–3148. [https://doi.org/10.1130/0016-7606\(1970\)81\[3141:potss\]2.0.co;2](https://doi.org/10.1130/0016-7606(1970)81[3141:potss]2.0.co;2)
- Krämer, K., Holler, P., Herbst, G., Bratek, A., Ahmerkamp, S., Neumann, A., et al. (2017). Abrupt emergence of a large pockmark field in the German Bight, southeastern North Sea. *Sci Rep-Uk*, 7(1), 5150. <https://doi.org/10.1038/s41598-017-05536-1>
- Lippmann, T. J. R., in 't Zandt, M. H., Van der Putten, N. N. L., Busschers, F. S., Hijma, M. P., van der Velden, P., et al. (2021). Microbial activity, methane production, and carbon storage in Early Holocene North Sea peats. *Biogeosciences*, 18(19), 5491–5511. <https://doi.org/10.5194/bg-18-5491-2021>
- Lohrberg, A., Schwarzer, K., Unverricht, D., Omlin, A., & Krastel, S. (2020). Architecture of tunnel valleys in the southeastern North Sea: New insights from high-resolution seismic imaging. *Journal of Quaternary Science*, 35(7), 892–906. <https://doi.org/10.1002/jqs.3244>
- Lundsten, E., Paull, C. K., Gwiazda, R., Dobbs, S., Caress, D., Kuhn, L. A., et al. (2024). Pockmarks offshore Big Sur, California provide evidence for recurrent, regional, and unconfined sediment gravity flows. *Journal of Geophysical Research: Earth Surface*, 129(5), e2023JF007374. <https://doi.org/10.1029/2023jf007374>
- Mayer, L. A., Raymond, R., Glang, G., Richardson, M. D., Traykovski, P., & Trembanis, A. C. (2007). High-resolution mapping of mines and ripples at the Martha's vineyard coastal observatory. *IEEE Journal of Oceanic Engineering*, 32(1), 133–149. <https://doi.org/10.1109/joe.2007.890953>
- Micallef, A., Averages, T., Hoffmann, J., Crutchley, G., Mountjoy, J. J., Person, M., et al. (2022). Multiple drivers and controls of pockmark formation across the Canterbury Margin, New Zealand. *Basin Research*, 34(4), 1374–1399. <https://doi.org/10.1111/bre.12663>
- Mueller, R. J. (2015). Evidence for the biotic origin of seabed pockmarks on the Australian continental shelf. *Marine and Petroleum Geology*, 64, 276–293. <https://doi.org/10.1016/j.margeo.2014.12.016>

- Murray, A. B., & Thieler, E. R. (2004). A new hypothesis and exploratory model for the formation of large-scale inner-shelf sediment sorting and "rippled scour depressions. *Continental Shelf Research*, 24(3), 295–315. <https://doi.org/10.1016/j.csr.2003.11.001>
- Özmaral, A., Abegunrin, A., Keil, H., Hepp, D. A., Schwenk, T., Lantzsich, H., et al. (2022). The Elbe Palaeovalley: Evolution from an ice-marginal valley to a sedimentary trap (SE North Sea). *Quaternary Science Reviews*, 282, 107453. <https://doi.org/10.1016/j.quascirev.2022.107453>
- Papenmeier, S., & Hass, H. C. (2020). Revisiting the Paleo Elbe Valley: Reconstruction of the Holocene, sedimentary development on basis of high-resolution grain size data and shallow seismics. *Geosciences*, 10(12), 505. <https://doi.org/10.3390/geosciences10120505>
- Paull, C., Ussler, W., Maher, N., Greene, H. G., Rehder, G., Lorenson, T., & Lee, H. (2002). Pockmarks off Big Sur, California. *Marine Geology*, 181(4), 323–335.
- Purser, A., Hehemann, L., Boehringer, L., Tippenhauer, S., Wege, M., Bornemann, H., et al. (2022). A vast icefish breeding colony discovered in the Antarctic. *Current Biology*, 32(4), 842–+. <https://doi.org/10.1016/j.cub.2021.12.022>
- Reusch, A., Lohrer, M., Bouffard, D., Moernaut, J., Hellmich, F., Anselmetti, F. S., et al. (2015). Giant lacustrine pockmarks with subaqueous groundwater discharge and subsurface sediment mobilization. *Geophysical Research Letters*, 42(9), 3465–3473. <https://doi.org/10.1002/2015gl064179>
- Scanlon, K. M., Coleman, F. C., & Koenig, C. C. (2005). Pockmarks on the outer shelf in the northern Gulf of Mexico: Gas-release features or habitat modifications by fish? *American Fisheries Society Symposium*, 41, 301–312.
- Schattner, U., Lazar, M., Souza, L. A. P., ten Brink, U., & Mahiques, M. M. (2016). Pockmark asymmetry and seafloor currents in the Santos Basin offshore Brazil. *Geo-Marine Letters*, 36(6), 457–464. <https://doi.org/10.1007/s00367-016-0468-0>
- Schmidt, C., Böttner, C., Schmidt, M., Müller, T. H., Wünsche, A., Willems, T., et al. (2021). Wave induced pockmark formation in the North sea, cruise No. MSM 99/2 (GPF 21-1_013), 26.03. 2021-05.04. 2021, Emden (Germany)-Emden (Germany). Helgoland pockmarks.
- Schneider von Deimling, J., Hoffmann, J., Geersen, J., Koschinski, S., Lohrberg, A., Gilles, A., et al. (2023). Millions of seafloor pits, not pockmarks, induced by vertebrates in the North Sea. *Communications Earth & Environment*, 4(1), 478. <https://doi.org/10.1038/s43247-023-01102-y>
- Seeberg-Elverfeldt, J., Koelling, M., Schlüter, M., & Feseker, T. (2005). Rhizon in situ sampler (RISS) for pore water sampling from aquatic sediments. *Abstracts of Papers American Chemical Society*, 230, U1763–U1764.
- Sommer, S., Linke, P., Pfannkuche, O., Schleicher, T., von Deimling, J. S., Reitz, A., et al. (2009). Seabed methane emissions and the habitat of frenulate tubeworms on the Captain Arutyunov mud volcano (Gulf of Cadiz). *Marine Ecology Progress Series*, 382, 69–86. <https://doi.org/10.3354/meps07956>
- Speller, R. (2000). Pock marks. In *Nearshore sands: Observations during Sandyduck97*.
- Szpak, M. T., Monteys, X., O'Reilly, S. S., Lilley, M. K. S., Scott, G. A., Hart, K. M., et al. (2015). Occurrence, characteristics and formation mechanisms of methane generated micro-pockmarks in Dunmanus Bay, Ireland. *Continental Shelf Research*, 103, 45–59.
- Venditti, J. G., Church, M. A., & Bennett, S. J. (2005). Bed form initiation from a flat sand bed. *Journal of Geophysical Research*, 110(F1). <https://doi.org/10.1029/2004jf000149>
- Wall, C. C., Donahue, B. T., Naar, D. F., & Mann, D. A. (2011). Spatial and temporal variability of red grouper holes within Steamboat Lumps Marine Reserve, Gulf of Mexico. *Marine Ecology Progress Series*, 431, 243–254. <https://doi.org/10.3354/meps09167>
- Watson, S. J., Neil, H., Ribó, M., Lamarche, G., Strachan, L. J., MacKay, K., et al. (2020). What we do in the shallows: Natura and anthropogenic seafloor geomorphologies in a drowned River Valley, New Zealand. *Frontiers in Marine Science*, 7. <https://doi.org/10.3389/fmars.2020.579626>
- Webb, K. E., Barnes, D. K., & Plankea, S. (2009). Pockmarks: Refuges for marine benthic biodiversity. *Limnology & Oceanography*, 54(5), 1776–1788. <https://doi.org/10.4319/lo.2009.54.5.1776>
- Whiticar, M., & Werner, F. (1981). Pockmarks: Submarine vents of natural gas or freshwater seeps? *Geo-Marine Letters*, 1(3–4), 193–199. <https://doi.org/10.1007/bf02462433>
- Wilkens, R. H., & Richardson, M. D. (2007). Guest editorial special issue on mine burial processes. *IEEE Journal of Oceanic Engineering*, 32(1), 1–2. <https://doi.org/10.1109/joe.2007.890937>
- Wright, J. P., & Jones, C. G. (2006). The concept of organisms as ecosystem engineers ten years on: Progress, limitations, and challenges. *BioScience*, 56(3), 203–209. [https://doi.org/10.1641/0006-3568\(2006\)056\[0203:tcooae\]2.0.co;2](https://doi.org/10.1641/0006-3568(2006)056[0203:tcooae]2.0.co;2)